R. & M. No. 3000
(13,997)
A.R.C. Technical Report

MINISTRY OF SUPPLY

AERONAUTICAL RESEARCH COUNCIL
REPORTS AND MEMORANDA

An Analysis of Available Data on the Local Aerodynamic Centres of Aerofoils in Two- and Three-Dimensional Flow

By

A. S. TAYLOR, M.Sc., A.F.R.AE.S.

LONDON: HER MAJESTY'S STATIONERY OFFICE
1957
FIFTEEN SHILLINGS NET

An Analysis of Available Data on the Local Aerodynamic Centres of Aerofoils in Two- and Three-Dimensional Flow*

By

A. S. TAYLOR, M.Sc., A.F.R.Ae.S.

COMMUNICATED BY THE DIRECTOR-GENERAL OF SCIENTIFIC RESEARCH (AIR), MINISTRY OF SUPPLY

Reports and Memoranda No. 3000†

January, 1951

Summary.—This report reviews existing information regarding the behaviour of the local aerodynamic centres of aerofoils, with a view to exposing the more important gaps in our knowledge, and indicating the lines along which future research might most profitably be directed.

Starting with the two-dimensional aerofoil in incompressible, viscous flow, for which aerodynamic centre position may be correlated with lift slope, the report passes on to examine the behaviour of the two-dimensional aerodynamic centre in compressible flow. Experimental data which have been analysed (relating to the subsonic and lower transonic régimes) are not in agreement with the predictions of potential flow theory; this suggests that the Reynolds number and transition position effects, associated with viscous flow, exert a powerful influence on the aerodynamic centre.

Considering next the locus of aerodynamic centres for wings of finite aspect ratio, the report discusses the various incompressible potential flow theories and their extension to the subsonic and transonic régimes of compressible flow, and collects in a series of figures, the published results of calculations by various investigators. A brief mention is made of supersonic theory. A further set of figures presents experimental data.

No prescription can be given for determining exactly the behaviour of the local aerodynamic centres of a given wing, but in the concluding section of the report it is suggested how the reader may use the assembled data to make a reasonable guess.

1. *Introduction.*—In a recent report[1] Gates has surveyed the present imperfect state of knowledge regarding movements of the overall aerodynamic centre of wing shapes likely to be used for transonic operation. Movements of the overall aerodynamic centre occur as the result of changes in the chordwise distribution of pressure—and hence of the local aerodynamic centre—at each section of the wing. In considering the basic stability of an aircraft (neglecting the effects of structural deformability) a knowledge only of the overall aerodynamic centre and not of the local aerodynamic centres of the wing is required. In general, however, within the speed range for which important movements of the overall aerodynamic centre occur, there will also be appreciable aero-elastic effects, to investigate which it is essential to know the loci of local aerodynamic centres, for the various incidence distributions (basic and incremental) relevant to the estimation of the various aerodynamic derivatives under consideration.

In the past it has been customary—for most numerical work, at least—to assume a fixed position for the aerodynamic ' axis ' (or locus of aerodynamic centres) corresponding to a constant chordwise position for the local aerodynamic centre, often identified with the quarter-chord point.

* Footnote, 1957. This analysis was made in 1950. No attempt has been made to incorporate data that have accrued since that date.

† R.A.E. Report Aero. 2407, received 10th May, 1951.

As long as wings remained unswept, and flight Mach numbers were well below the critical for the wing sections used, this assumption represented, in most instances, an acceptable approximation, although for certain wing sections the (low-speed) aerodynamic centre could differ from the quarter-chord point by as much as $0{\cdot}05c$.

When we come to consider wings of the shapes likely to be used for transonic operation we must, on theoretical and experimental grounds, reject the above assumptions. For, on the one hand, it will no longer be even approximately true that the aerodynamic centres of all sections lie at the same percentage of the local chord, while on the other hand, considerable movements of the aerodynamic ' axis ' will occur as the flow progresses from incompressible, through subsonic, to supersonic.

Ample theoretical or experimental evidence exists to support these general conclusions, but at the moment, theories are insufficiently developed and the experimental data too widely and unsystematically scattered over a vast field, to provide a sound basis for a method of predicting the position of the aerodynamic ' axis ' of a wing of given geometry under specified conditions of flight. In the present note, therefore, it is proposed only to indicate the general nature of the problem, to discuss the effects of some of the more important parameters involved, to examine the existing experimental data and to show where lie the more important gaps in our knowledge. The note should thus provide a basis for further discussion, and an indication of the lines along which future research in this field might most profitably be directed.

The problem can conveniently be considered in two parts:

(a) movements of the aerodynamic centre of an aerofoil in two dimensions,

(b) the effects of plan-form on the aerodynamic axis of a finite wing.

2. *Movements of the Aerodynamic Centre of an Aerofoil in Two Dimensions.*—2.1. *Aerodynamic Centre of an Aerofoil Section in Incompressible Flow.*—In a recent note[2], inspired by the pioneer work of Preston[3] at the National Physical Laboratory, Thomas has correlated the position of the aerodynamic centre of an uncambered or moderately cambered aerofoil with the rate of change of the lift coefficient with incidence. He obtains a relation of the type

$$\left(1 - \frac{h}{h_T}\right) = F(\tau)\left(1 - \frac{a_1}{a_{1T}}\right) \quad .. \quad .. \quad .. \quad .. \quad .. \quad .. \quad .. \quad (1)$$

where h is the position of aerodynamic centre, expressed as a fraction of aerofoil chord, and measured from the leading edge

a_1 is the rate of change of lift coefficient with incidence

τ is the trailing-edge angle of section

suffix $_T$ denotes the inviscid flow values of derivatives, with the Kutta-Joukowski circulation,

and the function $F(\tau)$ is independent of the type of aerofoil section, Reynolds number and transition point movement.

A curve of a_{1T} against thickness/chord ratio t/c is reproduced by Thomas from Ref. 4 and the ratio a_1/a_{1T} may be calculated using an experimental value of a_1 if known; alternatively, curves of a_1/a_{1T} against τ for various Reynolds numbers and transition point positions, reproduced from Ref. 5 may be used.

A curve of $F(\tau)$ against τ has been established from an analysis of American experimental results. $F(\tau)$ is shown to increase with τ and to be positive for $\tau > 3$ deg, although recent N.P.L. tests suggest that the curve should in fact, pass more nearly through the origin. Since a_1/a_{1T} is always less than unity, it follows that h is less than h_T; i.e., the aerodynamic centre in viscous flow is always ahead of its position in inviscid flow.

h_T can be shown to be given by a relationship

$$h_T \simeq h_T' \left\{ 1 + a\frac{t}{c} + b\tau \right\} \qquad \ldots \quad \ldots \quad \ldots \quad \ldots \quad \ldots \quad \ldots \quad (2)$$

where $h_T' = 0{\cdot}25$ or $0{\cdot}25 + 0{\cdot}28(t/c)^2$, according as τ (degrees) is greater than or less than $100t/c$, and where a, b are functions of maximum thickness position, which can be calculated from data given by Thomas, and shown to be positive for the usual range of positions of maximum thickness ($0{\cdot}25c$ to $0{\cdot}50c$).

From this work of Thomas, section thickness and trailing-edge angle, together with Reynolds number and transition position, emerge as the important parameters governing the aerodynamic centre position in two dimensional incompressible flow. The analysis leads to the following general conclusions:

(a) Scale and transition movement effects on aerodynamic centre are more marked for an aerofoil with a large trailing-edge angle than for an aerofoil with a small one, and transition movement effects are more important at low Reynolds number

(b) For a given t/c and a fixed transition position, the aerodynamic centre moves rearward as the Reynolds number increases

(c) For a given t/c and Reynolds number, the aerodynamic centre moves back as the transition position moves back.

As a corollary to (a) it may be deduced that

(d) Scale and transition movement effects are small in the case of aerofoils with concave trailing edges.

In examining the behaviour of the aerodynamic centres of a series of aerofoils as t/c increases, at given Reynolds number and fixed transition position, there are two opposing influences to be considered. On the one hand, since the coefficients a and b in equation (2) are positive, the theoretical aerodynamic centre position (inviscid flow) moves back as t/c increases. On the other hand, the effect of viscosity is to move the aerodynamic centre ahead of its theoretical position by an amount which is very small for small trailing-edge angles, but increases with increasing trailing-edge angle (and hence with increasing thickness for a given series of aerofoils). The net result may therefore differ according as the series under consideration has convex or concave trailing edges. Thus for the NACA symmetrical sections with convex trailing edges, considered later in this report (*see* Fig. 2) the low-speed aerodynamic centre moves forward with increasing t/c, while for the NACA 63-series aerofoils with concave trailing edges (*see* Fig. 11), it moves rearward.

A parallel investigation to that of Thomas has been made by Bryant, Halliday and Batson[6], using recent N.P.L. experimental results as a basis for curves of h/h_T against a_1/a_{1T}, for various trailing-edge angles. Although these curves do not exhibit the linearity of Thomas's correlation (equation (1) above), their application to aerofoils of practical importance leads to aerodynamic centre positions substantially in agreement with those obtained by Thomas's method.

2.2. *Aerodynamic Centre of an Aerofoil Section in Compressible Flow.*—2.2.1. *Theoretical.*—(a) *Subsonic* (*shock-free*).—According to Glauert's approximate thin-aerofoil theory, generalised in the 'N' similarity laws discussed by Dickson in Ref. 7, both C_m and C_L are increased in shock-free compressible flow by the factor $(1 - M^2)^{-1/2}$ and therefore there should be no effect on aerodynamic centre. Karman's formulae[8] for the pressures in compressible flow would indicate some movement of the aerodynamic centre with increasing Mach number but in most cases this would be small (*see* Ref. 9). A theoretical study by Kaplan[10] also indicates that little shift is to be expected at sub-critical Mach numbers.

(*b*) *Transonic.*—The 'N' similarity laws mentioned under (*a*) apply for sub-critical Mach numbers only, but another similarity law, applicable to transonic speeds, both below and above $M = 1$, can be formulated, and is discussed, for instance, by Spreiter in Ref. 11. This law, in its two-dimensional form, states that if we know the characteristics of one aerofoil of thickness-chord ratio (τ_0) as functions of M, in a transonic range, we can establish those of an aerofoil whose ordinates are those of the first multiplied by τ_1/τ_0 in a corresponding range of speeds. Corresponding speeds are given by

$$\beta_1 n^3 = \left(\frac{\tau_1}{\tau_0}\right) \beta_0 n^3 \quad \text{where } \beta = (|1 - M^2|)^{1/2}.$$

According to the theory (an essential assumption for which is that all the thickness/chord ratios involved should be small), the aerodynamic centres of the two sections at corresponding Mach numbers should lie at the same percentage of the respective chords from their leading edges.

(*c*) *Supersonic.*—For supersonic Mach numbers sufficiently in excess of $M = 1$ to make the assumptions of the linear perturbation theory valid, that theory shows the aerodynamic centre of a two-dimensional flat-plate aerofoil to lie at the half-chord point.

For aerofoils of finite thickness, the second-order theory of Busemann may be used to predict the position of the aerodynamic centre. Hilton discusses the limitations to the use of this theory in Ref. 12 and from the Busemann force coefficients quoted there*, it may be deduced that for doubly symmetrical aerofoils (as most commonly used for supersonic designs) the aerodynamic centre lies approximately at

$$c\left\{\tfrac{1}{2} - \frac{(\text{area of section})}{c^2} \frac{0{\cdot}6M^4 - (M^2 - 1)}{(M^2 - 1)^{3/2}}\right\}.$$

In particular, for a double-wedge of thickness ratio τ, it is approximately at

$$c\left\{\tfrac{1}{2} - \tau \frac{0{\cdot}3M^4 - 0{\cdot}5(M^2 - 1)}{(M^2 - 1)^{3/2}}\right\}$$

(*see* Ref. 13).

It will be remembered that, in incompressible flow, the aerodynamic centre is near to the quarter-chord point and that according to theory, little or no shift is to be expected in subsonic (shock free) compressible flow. Accordingly, to bring the aerodynamic centre back to its theoretical position, near the half-chord point in supersonic flow, a net rearward shift of approximately $0{\cdot}25c$ must occur in the transonic range. No theory has been advanced whereby the manner of the transition from the subsonic to the supersonic position can be predicted, although the transonic similarity law (*see* (*b*) above) provides a method of predicting the shift for a given aerofoil over a given Mach number range when the shift for a corresponding aerofoil over a corresponding Mach number range is known.

2.2.2. *Presentation of experimental data.*—The distance of an aerofoil section aerodynamic centre aft of a specified reference point in the section is given, as a fraction of the aerofoil chord, by the partial derivative $-\partial C_m/\partial C_L$, where the pitching-moment coefficient C_m is related to the given reference point. The parameters to be held constant in the differentiation are Mach number, Reynolds number and transition position. There has been a tendency in the past to regard the C_m—C_L relationship as a purely linear one, giving a constant value of the derivative $\partial C_m/\partial C_L$ and hence a unique position of the aerodynamic centre for a given Mach number, Reynolds number and transition position. In actual fact, C_m vs. C_L curves are seldom linear over more

* There appears to be an error in Hilton's paper; the integrals I_1, I_2, etc., should be rendered non-dimensional by substituting x/c for x.

than a very restricted C_L range and therefore in general, any quoted position for an aerodynamic centre is meaningless unless the associated value of C_L is given. In general, therefore, the aerodynamic centre position of a given aerofoil section must be regarded as a function of four variables: Mach number, Reynolds number, lift coefficient and transition position; if the Reynolds number is sufficiently large, the influence of transition position is negligible (*see* section 2.1) and the number of variables is reduced to three.

Experimental data appertaining to the position of the aerodynamic centre in compressible flow, which have been examined in the present investigation, exist in varying forms, from which the aerodynamic centre position can be obtained with varying degrees of accuracy.

Data are derived in some instances from force and moment measurements and in other cases from pressure-plotting experiments. Some of the reports have presented curves of dC_m/dC_L against Mach number, others have given C_m vs. C_L curves at various Mach numbers, while in a few cases, only the pressure distribution diagrams have been given, and it has been necessary to evaluate pitching-moment coefficients from these. In general, data have been available only in diagrammatic, and not tabulated form, and in view of the small scale of many of the diagrams, and of the inherent difficulty of measuring the slopes of curves accurately, no great accuracy can be claimed for the calculated aerodynamic centre positions.

The author has so far discovered no simple, and at the same time useful, method of correlating the data and it has thus seemed best to detail, in tabular form, the various sources of information, giving leading particulars of the aerofoil sections considered, the nature and conditions of the tests, and the form of presentation of the results. This has been done in Table 1, while the derived data on aerodynamic centre are presented in Figs. 1 to 21*. A discussion of the results follows in the next paragraph, but before proceeding to this, it is perhaps pertinent to observe that accurate agreement of the experimental results with the theory of section 2.2.1 is hardly to be expected, inasmuch as the theory relates to thin aerofoils in inviscid flow, whereas the experimental results relate to aerofoils of finite thickness and are subject to the influence of the Reynolds number and transition position effects associated with viscous flow. Thomas's paper[2] has shown how closely bound up is the aerodynamic-centre position in incompressible flow with the slope of the lift curve, which is itself much influenced by Reynolds number and transition position. Accordingly, when we consider compressible flow, any idiosyncrasies of behaviour of the lift slope are likely to be accompanied by corresponding idiosyncracies of behaviour of the aerodynamic centre. In this connection, it is unfortunate that in practically all the experimental work in this field, Mach number and Reynolds number have been varied simultaneously while no steps have been taken to define precisely the transition point.

2.2.3. *Discussion of experimental data.*—The only previous attempt to correlate experimental data, of which the author is aware, was that of Polhamus in Ref. 14. He selected thickness/chord ratio as the most influential parameter controlling the variation of aerodynamic centre location with M, and examined data for each of the three t/c ratios 6 per cent., 9 per cent., 12 per cent. Aerodynamic centre positions were determined from the slopes of the C_m vs. C_L curves in the low C_L range, all data being obtained at Reynolds numbers less than 2×10^6 with free transition. Shifts of aerodynamic centre relative to the position for $M = 0{\cdot}4$ were plotted against M for each t/c ratio, and two curves were drawn through the origin to define the limits of the measured shift for that t/c. From his results (Fig. 1 of Ref. 14, reproduced as Fig. 1 of the present paper) Polhamus concluded that:

(*a*) Forward or rearward movements of the aerodynamic centre as large as 12 per cent of the chord may occur

---

* *Note :* Aerodynamic-centre positions have usually been estimated for a specific C_L, approximately equal to the design C_L for the section, or as a mean value for a small range of C_L about this value. In many cases the estimated points showed a considerable degree of scatter, but to avoid confusion, only faired curves are shown in the figures.

(4999 A* 2

(*b*) For 6 per cent. thick aerofoils, the aerodynamic centre moves rearward with increasing Mach number while for thicker aerofoils (9 per cent and 12 per cent) it moves forward

(*c*) Aerofoils having thickness ratios of 7 per cent or 8 per cent might be expected to experience the least variations of aerodynamic centre with Mach number.

Polhamus's data appear to have been selected from a rather restricted field, excluding, for instance, the low-drag type of aerofoil with concave trailing edge. Moreover, the Reynolds number for many of the tests (*e.g.*, those of Refs. E.19 and E.20) was rather low. By no means all of the data examined in the present investigation fall within the appropriate boundaries of Fig. 1 and it must be questioned whether Polhamus has not attempted an over-simplification of the problem by exhibiting results in terms of the single parameter t/c. Such parameters as camber, position of maximum thickness, and trailing-edge shape appear to have a decided effect on the absolute position of the aerodynamic centre at a given Mach number, while the variation with Mach number certainly does not appear to be independent of those parameters. Accordingly the data analysed in the present report have, as far as possible, been cast into three main groups to show the effect of separately varying each of the parameters

I Thickness/chord ratio (t/c)

II Position of $(t/c)_{max}$

III Camber,

while group I has been subdivided into aerofoils with convex and concave trailing edges respectively. A fourth group has been reserved for data obtained from reports dealing with comparative tests of miscellaneous collections of aerofoils, exhibiting no systematic variation of the above parameters.

The range of experimental data falling into each group is shown in tabular form (Tables 2 to 5), each table being followed by a general discussion of the salient points emerging from an examination of the relevant figures. For fuller details of the aerofoil sections and of the conditions of test, reference should be made to Table 1; the various aerofoil notations involved therein, are explained in Ref. 15.

TABLE 2

Experimental Data Illustrating the Effect of Thickness-Chord Ratio

Item No.	Type of aerofoil	Thickness range (t/c)	Source of data Reference	Results given in Fig.
	(*a*) Aerofoils with convex trailing edge			
1	NACA Symmetrical; position of $(t/c)_{max}$ constant ..	6% to 18%	E.18	2, 3, 4
2	NACA Cambered; camber and position of $(t/c)_{max}$ constant.	9% to 21%	E.17, 15, 16(b), 17(b)	5, 6
3	NACA 16-Series. Several cambers; position of $(t/c)_{max}$ constant	6% to 21%	E.1	7
4	RAF 69 and 89. Camber and position of $(t/c)_{max}$ constant.	20·7% and 25%	E.8	8
	(*b*) Aerofoils with concave trailing edge			
5	NACA 63-Series; camber and position of $(t/c)_{max}$ constant.	6% to 12%	16, E.4	10, 11
6	H.S.1 and H.S.2; camber and position of $(t/c)_{max}$ constant.	15% and 12%	E.5	9

Discussion.—An examination of the figures indicates that in general, the aerodynamic centres of aerofoils with convex trailing edge tend initially to move forward as the Mach number increases, the forward trend being more pronounced, the thicker the aerofoil. These displacements are not in accordance with the linear Prandtl-Glauert theory or with the other theories mentioned in section 2.2.1, and as Göthert remarks in Ref. E.18b, it is evident ' that the formation of the boundary layer is decisive in causing the observed displacement of the aerodynamic centre '.

Figs. 2 and 5 suggest that for the thinner aerofoils (up to 12 per cent. thick) the forward trend will be reversed at, or about, the critical* Mach number, and the aerodynamic centre will move rapidly backwards. For the thicker aerofoils (as for instance the 15 per cent. and 18 per cent. thick symmetrical aerofoils of Fig. 2) a rapid forward movement may persist beyond the critical Mach number. From Göthert's pressure distribution diagrams it is clear that this divergent behaviour is due to the different ways in which the compression shock develops[E.18b]. Göthert anticipates, however, that the forward trend will eventually be reversed even with the thicker sections, and that at very high subsonic velocities the aerodynamic centre for all sections will have shifted to a position near the mid-chord point. Confirmation of the probability of an ultimate rearward shift is given by the results for NACA cambered aerofoils (Fig. 5) which bring out the additional fact, however, that further reversals of trend may occur, and give rise to large fluctuations of aerodynamic-centre position over quite small ranges of Mach number. Thus, for instance, the aerodynamic centre of the 23015 section, having initially moved forward from $0{\cdot}215c$ at $M = 0{\cdot}3$ to about $0{\cdot}195c$ at $M = 0{\cdot}65$, moves back to $0{\cdot}3c$ at $M = 0{\cdot}775$, then forward to about $0{\cdot}08c$ at $M = 0{\cdot}82$, and back again to $0{\cdot}47c$ at $M = 0{\cdot}85$.

The profound effect of the boundary layer, which invalidates the Prandtl-Glauert theory, is emphasised by an examination of Fig. 3 which shows the variation of lift slope, $\partial C_L/\partial \alpha_\infty$, with Mach number, for the five aerofoils under consideration. While the curves for the thinner aerofoils follow the theoretical curve fairly closely up to the critical Mach number, the curves for the 15 per cent and 18 per cent sections lie wholly below it; the 18 per cent section in fact shows a continuous decrease in $\partial C_L/\partial \alpha_\infty$ with increasing M.

An alternative method of presenting results for shift of aerodynamic centre (somewhat similar to that of Polhamus—Fig. 1) is illustrated in Fig. 4 for the NACA symmetrical aerofoils. Here the quantity plotted against Mach number is the shift of aerodynamic centre relative to the position in incompressible flow, as calculated by the method of Ref. 2, using for a_1 values extrapolated from the experimental results.

It will be noted that these results of Göthert in particular, and those relating to Table 2 in general, do not appear to be in very good agreement with Fig. 1 (Polhamus's correlation).

The analysis of the data appertaining to the cambered aerofoils (Item 2 of Table 2) provided an interesting check on the accuracy to be expected when aerodynamic centre positions are calculated from small-scale pressure distribution diagrams such as are given in Refs. E.16(a) and E.17(a). In the first instance, information on the 23009 and 23012 sections was available to the author only in the form of these pressure distribution diagrams, and C_m vs. C_L curves were obtained by graphical integration, aerodynamic-centre positions then being estimated by measuring the slopes of the curves. Subsequently, Refs. E.16(*b*) and E.17(*b*) came to hand, and it was possible to compare the present author's estimates with those of Göthert which should, of course, be the more accurate. The results of these independent estimates are compared in Fig. 6. There is reasonably good agreement as to the shape of the curves, but there are differences of as much as $0{\cdot}05c$ in the absolute position of the aerodynamic centre.

The NACA 16-Series aerofoils for which results are given in Fig. 7, are divided into three sets for each of which the design C_L, and hence the camber, is constant; the design C_L's are $0{\cdot}1$, $0{\cdot}3$ and $0{\cdot}5$ respectively and the corresponding cambers $0{\cdot}55$ per cent., $1{\cdot}65$ per cent. and $2{\cdot}76$ per cent. These results do not extend far beyond the critical Mach numbers, but generally speaking,

* The critical Mach number is here defined as the Mach number at which sonic velocity is just reached locally on the profile.

within the Mach number ranges considered, the broad trends observed above are followed. The behaviour of the 16–315 and 16–515 sections appears somewhat anomalous, however, in that the initial trend of the aerodynamic centre with increasing M is rearward instead of forward.

The results for the two thick aerofoils RAF 69 and 89 (Fig. 8) confirm the opinion that, although for such thick aerofoils, the initial forward trend of aerodynamic centre may persist beyond the critical Mach number, there will eventually occur a rapid rearward movement.

The two items of Table 2 which relate to aerofoils with concave trailing edge provide insufficient information upon which to base any definite conclusions as to the behaviour of such aerofoils.

The C_m vs. C_L curves for the NACA 63-Series low-drag profiles, to which Fig. 10 relates, were somewhat undulatory in character with, in most cases, no substantial linear portions, and in these circumstances it was decided to use the mean slope over the range $-0{\cdot}2 \leqslant C_L \leqslant 0{\cdot}6$ in determining the aerodynamic centre position. According to calculations by the method of Ref. 2, the aerodynamic centres of these aerofoils would, in incompressible flow, be expected to lie at about $0{\cdot}26c$. While at the lowest Mach number of the tests ($M = 0{\cdot}3$) the aerodynamic centres of the 6 per cent and 12 per cent sections approximate to this position, the aerodynamic centres of the 8 per cent. and 10 per cent. sections lie much further back ($0{\cdot}33c$ and $0{\cdot}305c$ respectively). There is no apparent explanation for the discrepancy; nor are these results supported by low-speed tests on aerofoils of the 63-Series, results of which are reproduced from Ref. 16, in Fig. 11 of this report.

Reverting to Fig. 10, it is seen that as M increases, the curves for the four profiles gradually converge to a value around $0{\cdot}30c$ at about $M = 0{\cdot}7$, beyond which the aerodynamic centres for all sections move rapidly rearward (with no reversals) to positions behind the mid-chord point.

It will be noted that for these aerofoils the aerodynamic centre was never ahead of the quarter-chord point in the Mach number range considered ($0{\cdot}3 \leqslant M \leqslant 0{\cdot}85$).

The high-speed aerofoils H.S.1 and H.S.2 which are respectively 15 per cent and 12 per cent thick, and have cusped trailing edges, exhibit practically no variation in position of the aerodynamic centre throughout the sub-critical Mach number range (*see* Fig. 9). At $M \simeq 0{\cdot}7$, there is evidence of a movement rearwards from the quarter-chord position, for both sections, but this is quickly reversed ($M \simeq 0{\cdot}74$) for the thicker aerofoil, while at $M \simeq 0{\cdot}78$, the aerodynamic centre of the 12 per cent thick section also begins to move rapidly forward. At the highest Mach numbers of the tests ($M = 0{\cdot}78$ and $0{\cdot}80$ respectively) the aerodynamic centre of each profile lies at about $0{\cdot}17c$. At still higher Mach numbers, the aerodynamic centres would presumably move rearwards again.

It will be observed that although groups 5 and 6 consist of aerofoils which are very similar, apart from the t/c range, the behaviour of the two sets of aerofoils appears to be quite different.

TABLE 3

Experimental Data Illustrating the Effect of the Position of $(t/c)_{max}$

Item No.	Type of aerofoil	Range of positions of $(t/c)_{max}$	Source of data Ref.	Results given in Fig.
1	NACA symmetrical, 12 per cent thick	30%c to 50%c	E.14	12
2	NACA symmetrical, 9 per cent. thick	20%c to 60%c	E.19	13

Discussion.—Besides differing in thickness, the two sets of aerofoils also differed as regards leading-edge radius, which was given in the case of the 12 per cent sections by $\varrho/c = 0{\cdot}55(t/c)_{max}^2$, and for the 9 per cent sections by $\varrho/c = 1{\cdot}1(t/c)_{max}^2$. Since, in the case of the 12 per cent thick sections, many of the relevant C_m vs. C_L curves (Fig. 15 of Ref. E.14) were markedly non-linear, it was decided to base ' mean ' aerodynamic centre positions for both sets of aerofoils, on the average rate of change of C_m over the range $0 \leqslant C_L \leqslant 0{\cdot}3$.

From Fig. 12, it will be seen that for the thicker aerofoils, pushing the maximum thickness rearward results in a more forward position of the aerodynamic centre at the lower Mach numbers, and also causes a more rapid forward movement with increasing M up to the value for which the reversed (rearward) trend sets in.

The same general tendencies are in evidence in Fig. 13 for the 9 per cent thick aerofoils. At least, this is true for the sections with $(t/c)_{max}$ at $0{\cdot}3c$, $0{\cdot}4c$ and $0{\cdot}5c$; but some qualification is necessary as regards the extreme positions of $0{\cdot}2c$ and $0{\cdot}6c$, for which the relevant curves are respectively further forward and further aft than would have been anticipated on the basis of extrapolation from the intermediate curves.

Qualitatively at least, the effect of rearward movement of $(t/c)_{max}$ is similar to that of increasing $(t/c)_{max}$ at a fixed chordwise position. This suggests that trailing-edge angle may be the most influential parameter entering the problem. The importance of trailing-edge angle in determining the form of the C_m vs. C_L curves, and hence the position of the aerodynamic centre, is confirmed by the results of some German tests (quoted in Ref. E.10) on three aerofoils, derived from the same basic section NACA 00012–0·55 50, by modification of the trailing portion so as to give trailing-edge angles $\tau = 31{\cdot}2$ deg (normal section), $17{\cdot}1$ deg and $6{\cdot}8$ deg respectively. The pitching-moment curves, which relate to a single Mach number ($M = 0{\cdot}5$) are reproduced in Fig. 14. It will be observed that the non-linearity of the pitching-moment curve in the region of $C_L = 0$, which is so pronounced for the normal section ($\tau = 31{\cdot}2$ deg), is substantially reduced for the intermediate section ($\tau = 17{\cdot}1$ deg) and has practically disappeared for the section with smallest trailing-edge angle ($\tau = 6{\cdot}8$ deg). The aerodynamic centre at low C_L, which is well forward for the normal section, moves progressively rearward with decreasing trailing-edge angle. The difference in aerodynamic centre position, as between the normal and the intermediate sections, is roughly the same as that between the normal section and the section 0 0012 0·55 30 whose (normal) trailing-edge angle is approximately equal to that of the intermediate 0 0012 0·55 50 section (*see* Fig. 12).

TABLE 4

Experimental Data Illustrating the Effect of Camber

Item No.	Type of aerofoil	Camber range (per cent)	Source of data Ref.	Results given in Fig.
1	NACA : $(t/c)_{max}$ = 12 per cent at 40 per cent c ..	0 to 4	E.11	15
2	NACA 16-Series; various $(t/c)_{max}$ at 50 per cent c ..	0 to 4	E.1	16 and 17

Discussion.—Although it is evident from Figs. 15 to 17, that the effect of camber on the variation of aerodynamic-centre position with Mach number, is considerable, it is difficult to perceive anything systematic in the manner in which the curves vary with increasing camber. In this connection it should be noted that in comparing sections of different camber (and hence of different design C_L's) some doubt must exist as to the most reasonable choice of C_L's on which to base the comparison.

The 12 per cent. thick aerofoils tested in Germany and discussed in Ref. E.11 are compared in Figs. 15a and 15b for low C_L (0 to 0·2) and for moderately high C_L (0·4 to 0·6). The differences

between the curves for the various cambers are more pronounced (particularly in the sub-critical range) at the low C_L than at the higher C_L; the critical Mach numbers, it will be noted, are more widely spaced in the former case than in the latter.

A C_L range from 0·2 to 0·4 was selected for the comparison of the 9 per cent and 12 per cent thick NACA 16-Series aerofoils (Fig. 16) since this seemed to avoid the grosser non-linearities of the relevant C_m vs. C_L curves. Fig 17a deals with the NACA 16-X15 aerofoils over the same C_L range; in this case, the non-linearities were not so consistently avoided—a fact which is reflected in the extremely wide variations of aerodynamic centre position exhibited in this figure. In Fig. 17b the 15 per cent aerofoils are again compared, the aerodynamic centre positions for each aerofoil being derived in this case from the mean slopes of the C_m vs. C_L curves in the C_L range extending 0·1 on either side of the design C_L for the section. In this way the worst non-linearities were avoided and the excursions of the aerodynamic centre correspondingly restricted.

TABLE 5

Miscellaneous Experimental Data

Item No.	Type of aerofoil	Remarks	Source of data Ref.	Results given in Fig.
1	*Mustang* low-drag aerofoil	Comparative R.A.E. and N.P.L. tests.	E.6	18
2	0 0012–0·55 50 and E.C. 1250	These sections are to all intents and purposes, identical.	E.12 E.9	19 and 20
3	Miscellaneous collections of unrelated N.A.C.A. aerofoils.		(*a*) E.2 (*b*) E.3	21(a) 21(b)

Discussion.—Items 1 and 2 have been included mainly to illustrate the difficulties which beset the would-be correlator of data on aerodynamic centre when such data are collected from a variety of sources.

The curves of Fig. 18 relating to the *Mustang* low-drag wing section* were derived from independent sets of pressure distribution measurements made respectively at the R.A.E. and N.P.L. In the R.A.E. tests the Reynolds number was kept nearly constant at 2×10^6 while in the N.P.L. tests, it varied from about $1{\cdot}1 \times 10^6$ at $M = 0{\cdot}4$ to $1{\cdot}8 \times 10^6$ at $M = 0{\cdot}8$; transition occurred at $0{\cdot}3c$ on the R.A.E. model and at $0{\cdot}6c$ on the N.P.L. model. As will be seen from the figures, the two sets of tests indicate quite different characteristics for the aerodynamic centre vs. M curve.

A comparison of the ordinates of the two sections listed as Item 2, shows them to be, to all intents and purposes, identical, but although both sets of results afford qualitative confirmation of the deductions made in the discussion of Table 3—that a large trailing-edge angle is conducive to a forward position of the aerodynamic centre at low M, and to a rapid forward movement (initially) with increasing M—there are quantitatively large differences in the behaviour of the aerodynamic centre (Fig. 19) and of the lift slope (Fig. 20). The large differences between the aerodynamic centre curves of each aerofoil for $C_L = 0$ and $C_L = 0{\cdot}2$ respectively, are due to the marked non-linearity of the C_m vs. C_L curves near $C_L = 0$, a feature previously observed for the 0 0012–0·55 50 section in the discussion of Table 3, where the effect of reduced trailing-edge angle in eliminating such non-linearities was also noted (*see* Fig. 14).

* Models for both the R.A.E. and the N.P.L. tests were copied from templates of the full-scale wing which differed considerably from the ideal section.

Beyond emphasising how widely divergent may be the behaviour of the aerodynamic centres of different types of aerofoil, Figs. 21a and 21b provide no information of particular significance. It should be noted that aerodynamic centres for the set of aerofoils featured in Fig. 21a were derived from the curves of $\partial C_{m c/4}/\partial C_n$ vs. M given in Fig. 55 of Ref. E.2, on the assumption that, for the low values of C_L considered, the difference between $\partial C_{m c/4}/\partial C_n$ and $\partial C_{m c/4}/\partial C_L$ would be negligible.

2.2.4. *Experimental data for the transonic and supersonic régimes.*—Most of the tests discussed in the preceding section have extended beyond the subsonic régime into the lower end of the transonic régime. Few, if any, however, have been carried up to Mach numbers sufficiently near 1·0 for the transonic similarity law of section 2.2.1(*b*) to hold. At any rate, such groups of related aerofoils as the NACA 63-Series, for which results are given in Fig. 10, do not appear to behave in accordance with the law over the highest part of the Mach number range considered; the curves are in fact, less widely spaced than would be predicted.

There seem, as yet, to be no reliable experimental data appertaining to the upper part of the transonic régime or to the supersonic régime.

3. *The Locus of Aerodynamic Centres for Wings of Finite Aspect Ratio.*—3.1. *Incompressible Potential Flow Theories.*—The exact theoretical determination of the locus of local aerodynamic centres for a wing of finite aspect ratio in non-viscous, incompressible flow, forms part of the more general problem of determining the load distribution for such a wing. This involves the solution of a difficult three-dimensional potential flow problem which has for many years occupied the attentions of numerous investigators. Before the advent of the swept-back wing, Prandtl had introduced the conception of the 'lifting line' in an attempt to avoid some of the difficulties, but while lifting-line theory can cope, without undue loss of accuracy, with nearly straight wings of fairly large aspect ratio, it is quite inadequate in dealing with present-day wing shapes. In presenting his own approximate solution of the problem, Multhopp[17] has briefly reviewed other methods of approach, of which we may here mention those of Schlichting and Kahlert[18], Falkner[19, 20, 21] and Garner[22, 23], together with that recently put forward by Küchemann[26].

Although it represents a step towards the true lifting-surface conception, the method of Schlichting and Kahlert is virtually only a modified extension of the lifting-line conception, involving the replacement of continuous vorticity by a number of kinked lifting lines distributed chordwise, and each having a continuous spanwise load distribution; the downwash singularity at the kink of a typical vortex line, whose vorticity is expressed by a Fourier series, is dealt with by adding a 'middle function' to the Fourier expansion. This approach has given promise of providing a reasonably accurate and not too laborious method of predicting the chordwise load distribution (and hence local aerodynamic-centre position) of straight and swept wings, but the ultimate development of the method is at present held up by difficulties concerning the 'middle function'*.

The principles of Falkner's vortex-lattice theory were introduced in Ref. 19, and the methods by which they may be applied to the calculation of the aerodynamic loading of wings by lifting-plane theory, are described in detail in Ref. 20, which introduces the so-called P functions into the loading formula for the vortex sheet representing the wing, to cope with the sudden changes of direction of the leading and trailing edges of a tapered wing at the centre-line. The scope of the latter paper is limited to the application of the general principles, to symmetrical incidence solutions and to symmetrical and anti-symmetrical wing-twist solutions. A set of solutions for a delta (equilateral triangle) wing is given. In a further report[21], Falkner has collected together the aerodynamic loadings due to incidence of a number of straight and sweptback wings, as calculated by the method of Ref. 20.

---

* *Footnote added* 1957.

The position regarding the Schlichting method is unchanged. Following the successful introduction of the Multhopp method (R. & M. 2884), attempts to resolve the difficulties which had arisen with the former method were discontinued.

Garner and Multhopp have both attempted to operate with a continuous lifting surface, avoiding some of the physical or mathematical assumptions which characterise the other approaches, but whereas the former's method is far too laborious to use for routine calculations, Multhopp's is reasonably economic as regards computor labour. The proposals put forward by Garner in Ref. 22 have been applied by him, in Ref. 23, to the calculation of the aerodynamic load distribution on a delta wing, while Multhopp's method is set out in full with worked examples in Ref. 17.

In Ref. 26, Küchemann has put forward a semi-empirical solution of the problem, which entails only a fraction of the computer-labour involved in the other methods. As a method of calculating the locus of local aerodynamic centres, it must be treated with some reserve, since it empirically specifies the chordwise loading for each spanwise station of the wing at the outset. Thus, the chordwise loading over the middle of the semi-span of a wing of sweep angle ϕ, is assumed to be that of a flat plate, with a local lift slope $a = 2\pi \cos \phi$, while at the centre, a formula for the chordwise loading, depending on sweep angle, but independent of aspect ratio, is derived from an analysis of the infinite aspect ratio wing with constant spanwise loading. The local lift slope and aerodynamic centre are then also expressed in terms of sweep angle only. The tip region is assumed to behave like the centre portion of a swept-forward wing and accordingly, the results for the centre are applied, with the sign of the sweep reversed. Finally, to link up the results for the centre and tip with those for the middle of the semi-span, an empirical curve, based on a number of experimental results of pressure plotting on swept wings, is used.

From examples quoted for wings of aspect ratio 3 and upwards, the method would appear to give good agreement with experiment, and reasonable agreement with other methods of calculation. For very low aspect ratio, however, loci of aerodynamic centres derived by this method would evidently not agree with those deduced by Falkner (*see* Fig. 22). Nor would this method predict the shape of the aerodynamic centre loci, obtained by other methods of calculation, for distributions of twist at zero lift (*see* Figs. 27, 28 and 29d).

3.1.1. *Numerical results.*—Results of calculations by the methods mentioned above, which are relevant to the present investigation, are collected together in Figs. 22 to 28, upon which the following comments may be offered.

(*a*) *Constant-chord wings at uniform incidence :* Falkner's calculations (Figs. 22 and 23) indicate the following points:

(i) For an unswept wing of fairly large aspect ratio, the local aerodynamic centre lies very close to the quarter-chord point at the wing root, but shows a continuous forward tendency on moving outwards towards the tip, where it may be some 4 per cent of the chord further forward

(ii) As aspect ratio is decreased, the locus of aerodynamic centres moves bodily forward, while retaining the same general shape

(iii) Sweeping a wing back, while maintaining constant aspect ratio, tends to send the local aerodynamic centre further back at the root and to bring it forward at the tip.

(*b*) *Delta and cropped delta wings at uniform incidence :* Fig. 24 gives the results of Falkner's calculations for a triangular wing of 90-deg apex angle (aspect ratio = 4) and for wings of aspect ratio 3 and 2·309 respectively, obtained from it by cropping the tips. Reduction in aspect ratio (which also, of course, involves a change of taper) tends to bring the local aerodynamic centre forward over the whole span, but the effect is most pronounced towards the tip.

Garner, Multhopp and Küchemann have also made calculations for the cropped delta of aspect ratio 3·0 and their results are compared with Falkner's in Fig. 25, which indicates reasonable agreement except near the tip.

Fig. 28 gives Falkner's results for a delta wing of 60-deg apex angle, while Fig. 26 gives the results of calculations carried out in Sweden by Berndt and Örlik-Rückemann[24] for delta wings of apex angles 64 deg, 45·2 deg and 28·2 deg, and also for cropped delta wings of taper ratio

0·303 derived therefrom. The method used is that of Falkner, employing a basic layout of 126 vortices with six control points, two additional control points in the root section being introduced for the calculation of a correcting distribution which allows for the discontinuity of the leading edge.

From Fig. 26a it is seen that for the delta wing of largest aspect ratio considered ($A = 2{\cdot}50$), the local aerodynamic centre moves forward on going from the root towards the tip, this tendency being reversed, however, over the last 20 per cent or so of the span. Reduction of aspect ratio (and apex angle) moves the whole locus rearward and accentuates the rearward-moving tendency towards the tip.

For cropped deltas (Fig. 26b) there is less difference between the loci for the different aspect ratios and unlike the pure deltas, there is no rearward-moving tendency towards the tips.

(*c*) *Wings with linear distribution of twist at zero lift :* In many aero-elastic problems, we are concerned with a basic lift distribution corresponding to uniform incidence, together with an incremental lift distribution (of zero total lift) corresponding to an arbitrary mode of twist. The locus of aerodynamic centres for the twist distribution will be quite different from that corresponding to uniform incidence, as can be seen from Figs. 27 and 28, which give the results of calculations for uniform incidence and linear twist, carried out by the methods of Multhopp* and Falkner respectively, for a tapered swept-back wing and a delta wing of apex angle 60 deg. It will be seen that the loci corresponding to the twist distributions exhibit infinite discontinuities towards the mid-semispan, the inboard and outboard branches running off to infinity in the forward and rearward directions respectively.

3.2. *Extension of the Theories to Subsonic Compressible Flow.*—Within the limitations of the linearised theory, the incompressible flow theories of section 3.1 may be extended to the subsonic régime of compressible flow, by application of the three-dimensional form of the similarity laws mentioned in section 2.2.1. This states[7] that the compressible flow (Mach number M) round a wing A corresponds to an incompressible flow round a wing B whose longitudinal dimensions are those of A, but whose lateral dimensions are in the ratio $\beta : 1$, whilst the normal dimensions are in the ratio $\beta^{N-1} : 1$, to those of A ($\beta = \sqrt{(1 - M^2)}$). The local aerodynamic centre at a given spanwise location of wing A, at Mach number M, will thus lie at the same percentage of the local chord as does the local aerodynamic centre at the corresponding spanwise location of wing B in incompressible flow.

The results of applying the similarity law to wings of various plan-forms are shown in Fig. 29, in the derivation of which, use was made of some of Falkner's results. The general effect of compressibility on the locus of aerodynamic centres for wings at uniform incidence appears to be to move it rearwards at the root and to increase the (negative) slope from root to tip. These two factors exert opposing influences on the aerodynamic centre at the tip which accordingly, may in some cases be further forward in compressible flow than in incompressible flow, and in other cases further aft.

The one case of twist for which results are given (Fig. 29d) indicates a forward movement of the inboard branch of the locus and a rearward movement of the outboard branch, due to compressibility.

3.3. *Behaviour in the Transonic Range.*—The similarity law of the preceding section applies for sub-critical Mach numbers only, and it is thus not possible to make a direct calculation of aerodynamic-centre positions for a given wing at transonic Mach numbers. If, however, the locus of aerodynamic centres for a certain wing is known for specified Mach numbers within the transonic range, then by application of the three-dimensional form of the transonic similarity law mentioned in section 2.2.1, the locus, can, in theory, be determined for an infinite family of related wings at transonic Mach numbers corresponding to (but not identical with) the original set.

* Fig. 27 also shows Küchemann's results for the uniform incidence case.

The family of equivalent wings may be defined as follows[11]:

Let A, τ be the aspect ratio and thickness/chord ratio respectively, of a member of the family whose aerodynamic characteristics are known at a certain transonic Mach number M and let $\beta = (|1 - M^2|)^{1/2}$. Then if M' be a second (arbitrary) transonic Mach number and $\beta' = (|1 - M'^2|)^{1/2}$, the member of the family corresponding to this Mach number is obtained by multiplying the normal and lateral dimensions of the first wing by $(\beta'/\beta)^3$ and β/β' respectively. The aspect ratio A' and thickness/chord ratio τ' of the second wing are thus given by

$$A' = \frac{\beta}{\beta'} A \,, \qquad \tau' = \left(\frac{\beta'}{\beta}\right)^3 \tau$$

and its aerodynamic characteristics at Mach number M' may be deduced from those of the first wing at Mach number M. In particular,the chordwise position of the local aerodynamic centre at a given spanwise location will be the same for the two wings at the corresponding Mach numbers.

3.4. *Supersonic Theory.*—In Ref. 1, Gates has referred in some detail to Puckett's and Stewart's supersonic conical solution for the lift distribution of wings with pointed tips, and in Fig. 9 of his paper (reproduced as Fig. 30 of the present report) he gives the loci of local aerodynamic centres, appropriate to the external* solution, for wings of various plan-forms.

From Fig. 30 it is seen that for pointed wings, operating with conical flow inside the Mach cone, the local aerodynamic centre lies at the mid-chord point at the root, and tends to a position one-third of the chord behind the leading edge towards the tip. At intermediate spanwise positions, the aerodynamic-centre location depends on the value of the parameter δ defining the wing shape (*see* figure); it moves progressively forward as δ increases from negative values (lozenge-shape wings), through zero (delta wing), to positive values (arrow-head wings).

3.5. *Experimental Data.*—It will be evident that in order to provide a satisfactory experimental check on the validity of the theories discussed in sections 3.1 to 3.4, it would be necessary to carry out comprehensive pressure-plotting tests over a wide speed range on a variety of wing shapes, embracing all those combinations of aspect ratio, taper ratio and sweepback, likely to be encountered in practice. At the same time, calculations would have to be performed on the same set of wings in accordance with the relevant theories. No such complete programme of work has so far been undertaken, nor, with available resources, is it likely to be. The N.P.L. has embarked on a modest programme of work on a family of arrow-head wings with quarter-chord line swept back 45 deg. The basic half-wing model with pointed tip, corresponding to aspect ratio 6 for the complete wing, will be so constructed that the span may be progressively reduced to give aspect ratios of 3·82, 2·64 and 1·71 for the complete wing†. The wing section is to be RAE 102 with maximum thickness of 10 per cent at 0·35 chord. Experimentally determined load distributions will be compared with those calculated by the various theoretical methods.

Existing experimental data on the locus of aerodynamic centres for wings of finite aspect ratio are collected together in Figs. 31 to 42 and are commented on in sections 3.5.1 to 3.5.4. As in the case of the two-dimensional data, it must be stressed that complete agreement of the experimental results with the theoretical is hardly to be expected since the theory relates to thin

---

* There are two régimes for conical flow over a delta wing; one, in which the Mach cone is outside the wing surface is called the *external* solution, the other, in which the Mach cone intersects the surface, is called the *internal* solution. These solutions can be applied to more general shapes with pointed tips, provided that the Mach cones springing from the tips and the rear end of the root chord do not cut the wing.

At the time this report was written, the external solution appeared to be the more important for practical design application and no attempt was, therefore, made to calculate aerodynamic-centre positions corresponding to the more complicated internal solutions.

† In the notation of Ref. 1, the four wings are given by $(\delta, \lambda) = (3/4, 0)$, $(3/4, 2/9)$, $(3/4, 7/18)$ and $(3/4, 5/9$ respectively.

aerofoils in potential flow while the experimental results relate to aerofoils of finite thickness, and are subject to the influence of the Reynolds number and transition position effects associated with viscous flow. With regard to compressibility effects in the subsonic régime, we have already seen how, in practice, large movements of the two-dimensional section aerodynamic centre occur in contradiction to the linear theory. Accordingly it would be surprising if, in three dimensions, movements of the local aerodynamic centres were to be strictly in accordance with the similarity law of section 3.2.

3.5.1. *Low-speed tests of constant-chord swept-back wings* (*Figs.* 31 *and* 35).—(*a*) Fig. 31 gives a comparison of experimental and theoretical results for two constant-chord swept-back wings tested in the No. 2 $11\frac{1}{2}$-ft Wind Tunnel of the R.A.E.[E.21, 22] at low Mach number. Agreement is tolerably good, bearing in mind that the effect of finite thickness on the two-dimensional section aerodynamic centre is to move it forward of the theoretical (thin aerofoil) position.

For the wing of aspect ratio 5 and sweepback 45 deg (Fig. 31a), the experimental locus of aerodynamic centres is somewhat flatter over the middle portion of the semispan than the theoretical curve derived from Falkner's calculations, but agrees rather better with Küchemann's calculation.

For the smaller aspect ratio wing of sweepback 53·1 deg (Fig. 31b) an interesting feature is the way in which the experimental locus for the wing with square tip departs from the theoretical curve towards the tip. The pronounced rearward trend towards the tip is ascribed by Weber[E.22] to an ' end-plate effect ' associated with the assumption of a vortex sheet which runs up the edges of the wing. This feature is not exhibited by the wing with rounded tip, at the lift coefficient considered, but Weber suggests that in this case the effect will show at larger incidences.

(*b*) Fig. 35 gives the results of a comparison carried out by Holme[E.23] in Sweden, between two constant-chord wings of aspect ratio 4·5, one unswept and the other swept back at 40 deg. Experimental results are compared with the results of calculations based on Holme's own approximate solution of the lifting-surface problem, which replaces the wing by two discrete vortices along the $\frac{1}{8}c$ and $\frac{5}{8}c$-lines and determines their strengths by the condition of zero normal velocity at points on two control lines, at $\frac{1}{2}c$ and $\frac{3}{4}c$ respectively. It should be noted that the figure presents the loci of centres of pressure which, since the aerofoil section is symmetrical, should differ little from the loci of aerodynamic centres.

3.5.2. *Low-speed tests of delta wings* (*Figs.* 25, 26, 32 *and* 33).—

(*a*) On Fig. 25 are shown experimental points, deduced from the unpublished results of pressure-plotting experiments at the N.P.L., on the cropped delta wing of apex angle 90 deg and aspect ratio 3·0, which was the subject of the comparative calculations mentioned in section 3.1.1 (*b*). Agreement with theory is very good over the inboard half of the semispan, but towards the tip, the forward trend predicted, in varying degree, by the various theories, is not reproduced.

(*b*) Another delta wing of aspect ratio 3, but with apex angle 84 deg, has been tested in the 5-ft Open Jet Wind Tunnel at the R.A.E.[E.24], and results for local centres of pressure at two incidences are reproduced in Fig. 32 together with the local aerodynamic-centre positions deduced therefrom, and also a theoretical curve estimated by interpolation in the results of Refs. 21 and 25 (Falkner). The experimental points exhibit a fair degree of scatter, and the mean curves of centre of pressure for the two incidences differ considerably from one another and also from the locus of aerodynamic centres deduced from them and the corresponding spanwise lift distributions.

(*c*) Of the delta and cropped delta wings which were the subjects of the calculations reported in Ref. 24, two have been tested in a wind tunnel, and results are shown in Fig. 26 for comparison with the calculated values. Agreement is seen to be fair over the inboard half of the semispan, but to become progressively poorer towards the tip, where the experimental aerodynamic centres lie well behind the calculated positions.

(*d*) Ref. E.25 gives section lift curves and the spanwise variation of local centre of pressure over a wide range of angles of attack for a triangular wing of aspect ratio 2·0 (apex angle 53 deg 8 min) tested at low Mach number in America. From these results, curves of spanwise variation of aerodynamic centre have been deduced for mean lift coefficients ($\bar{C}_L$) of 0·2 and 0·5 respectively, and these are reproduced in Fig. 33, which also shows the theoretical curve for an equilateral triangle (aspect ratio 2·31, apex angle 60 deg), as given in Fig. 28. The experimental curve for $\bar{C}_L = 0{\cdot}2$ lies fairly close to the theoretical curve, the greatest discrepancy being at the root where the experimental aerodynamic centre is about $0{\cdot}40c$ ahead of the theoretical. At the higher lift coefficient ($\bar{C}_L = 0{\cdot}5$), the complete locus has moved rearwards by a considerable amount, while towards the tip, the usual forward trend of aerodynamic centre is reversed, and a marked rearward movement is observed.

3.5.3. *Low-speed tests of arrow-head wings* (*Figs.* 34 *and* 36).—

(*a*) Ref. E.26 gives the results of Swedish pressure-plotting tests on a 2 : 1 tapered wing of aspect ratio 4·5, with quarter-chord line swept back at 40 deg. The results are in the form of local normal force coefficients C_n and local centre of pressure positions over a wide range of incidence. The centre of pressure positions for $\alpha = 5$ deg are plotted in Fig. 34 of the present report, together with an approximate assessment of local aerodynamic centres, at a mean lift coefficient $\bar{C}_L \simeq 0{\cdot}2$, deduced from the slopes of C_m vs. C_n curves derived from the given data. The centre of pressure curve is of the general shape predicted by theory for such a wing (compare Fig. 27 which relates to a wing of somewhat similar proportions); the locus of aerodynamic centres is rather erratic in comparison.

(*b*) Ref. E.27 gives local lift and pitching-moment coefficients at a number of spanwise stations of a 4 : 1 tapered wing of aspect ratio 3·61 and sweepback 59 deg, obtained from pressure-plotting experiments in the No. 2 11½-ft Wind Tunnel of the R.A.E. From these, the locus of aerodynamic centres shown in Fig. 36, for a mean lift coefficient $\bar{C}_L \simeq 0{\cdot}1$, has been derived. Tolerably good agreement is shown with the theoretical curve of Falkner[25], and rather better agreement with Küchemann's results[26].

3.5.4. *High-speed tests and compressibility effects.*—

(*a*) According to the Similarity Law of section 3.2, the 59-deg sweptback wing illustrated in Fig. 36, which was the subject of low-speed tests, reported in Ref. E.27, is the equivalent in incompressible flow, of a 4 : 1 tapered wing of aspect ratio 5·87 and sweepback 45 deg in compressible flow at $M = 0{\cdot}8$. Such a wing has been tested in the R.A.E. High Speed Tunnel at Mach numbers up to about 0·91, and the unpublished results include local C_m vs. C_L curves for four spanwise locations on the wing at various Mach numbers and also curves showing the variation of local centre of pressure position with Mach number, for each section, at two angles of attack. From the slopes of the C_m vs. C_L curves for $M = 0{\cdot}8$, the locus of aerodynamic centres at a mean lift coefficient $\bar{C}_L \simeq 0{\cdot}1$ has been deduced and is compared in Fig. 37 with the low speed curve for the equivalent* wing, taken from Fig. 36. Agreement is seen to be quite good, except very near the tip.

The C_m vs. C_L curves for Mach numbers above $M = 0{\cdot}8$ are completely non-linear and no attempt has therefore been made to derive aerodynamic-centre positions from them. Fig. 40, however, presents the spanwise variation of centre of pressure at small incidence ($\alpha = 2{\cdot}1$ deg) for Mach numbers from 0·6 to 0·915. Up to $M = 0{\cdot}872$, the effect of increasing Mach number is to increase the general slope of the locus of centres of pressure by moving it rearward over the inner part of the semispan and forward over the outer part; movements are relatively small. This increase in slope is in qualitative agreement with predictions based on the subsonic similarity law (*see* Fig. 29c) although theory indicates a rearward movement with increasing Mach number over the whole span. The crossing over of the experimental curves for different Mach numbers

* The two equivalent wings have the same thickness-chord ratio so that the relevant value of N in the similarity law (*see* section 3.2) is $N = 1$.

is, in fact, similar to that calculated for a constant-chord wing (*see* Fig. 29b). Above $M = 0{\cdot}87$, much larger shifts of centre of pressure occur than would be predicted using the similarity law*; these presumably correspond to the large shifts of section aerodynamic centre which occur in two-dimensional flow at Mach numbers above the critical.

(*b*) The delta wing of Fig. 25 ($A = 3$, apex angle 90 deg) has, in association with a body, been pressure plotted in the High-Speed Wind Tunnel of the R.A.E. at Mach numbers from 0·40 to 0·92[E.28]. Curves of local aerodynamic-centre variation deduced from these experiments are given in Fig. 38 which also shows Falkner's theoretical curve for the wing alone, in incompressible flow.

(*c*) Fig. 39 shows the approximate spanwise variation of aerodynamic centre for a 2 : 1 tapered wing of aspect ratio 6 with half-chord line unswept, as deduced from American tests[E.29] at various Mach numbers. The curves shown, which relate to a mean lift coefficient $\bar{C}_L \simeq 0{\cdot}2$, appear somewhat erratic and no systematic variation with Mach number is discernible.

(*d*) Fig. 41 relates to American tests[E.30] of a wing which, when unswept, has an aspect ratio of 9·0 and a taper ratio of 2·5 : 1·0. In conjunction with a typical fuselage, the wing was tested with no sweep, and also with 30 deg and 45 deg of sweepback and sweepforward, at Mach numbers from 0·60 to 0·96. Sweep was obtained by rotating the wing semispans about a point in the plane of symmetry; pressure-plotting stations, which lay perpendicular to the quarter-chord line of the unswept wing, rotated with it. The various test configurations are illustrated in Fig. 42. In Ref. E.30, test data are given in the form of normal force coefficients (c_n') of sections perpendicular to the unswept quarter-chord line, and twisting-moment coefficients (c_t) of such sections about that line. The ' aerodynamic-centre ' positions plotted in Fig. 41 relate to sections perpendicular to the unswept quarter-chord line and have been derived from the expression

$$h_\phi = 0{\cdot}25 - \frac{\Delta c_t}{\Delta c_n'}$$

where $h_\phi c_\phi$ is the distance of the point in question behind the leading edge of the section, the chord of which is denoted by c_ϕ, and Δc_t, $\Delta c_n'$ are increments of twisting-moment and normal-force coefficients corresponding to a given increment $\Delta\alpha$, of wing angle of attack.

In general, therefore, the point in question is not a true aerodynamic centre; in the case of the unswept wing (if the difference between normal force and lift coefficients at moderate incidence is neglected), it represents a mean aerodynamic centre corresponding to the angle of attack increment $\Delta\alpha$.

Nevertheless, h_ϕ is quite a convenient parameter to employ in a comparison of the effects of compressibility on chordwise pressure distribution for wings of various sweep angles.

Fig. 41a shows that for the unswept wing of large aspect ratio, the locus of aerodynamic centres which, at $M = 0{\cdot}6$, varies little from a mean position of about $0{\cdot}21c$ across the span, has moved bodily rearwards by some $0{\cdot}20c$ at $M = 0{\cdot}89$; further increase of M to 0·925 produces relatively little change.

Figs. 41b to 41d illustrate how such rearward movement of the aerodynamic centres may be delayed by sweeping the wing either forward or back. The wing of 45 deg sweepforward exhibits the smallest variations of aerodynamic-centre position over the range of Mach numbers from 0·6 to 0·96.

For the wing of 45-deg sweepback, the ' aerodynamic centre ' appears surprisingly far back towards the tip; this is probably accounted for by the fact that at the higher of the two angles of attack (10 deg) on which the derivation is based, the tip sections of the wing were stalled. Data for an intermediate angle of attack were not available.

* This statement has not been checked by detailed calculations for the equivalent wings appropriate to the higher Mach numbers, but there can be little doubt of its truth having regard to the small differences in plan-form of these wings.

3.5.5. *Experimental data for the transonic and supersonic régimes.*—Some of the tests mentioned in the preceding section have extended into the lower end of the transonic régime and it has been observed how, as the Mach number approaches 1·0, the locus of aerodynamic centres eventually moves back by amounts in excess of what would be predicted by the subsonic similarity law. As far as the author is aware, however, no transonic experimental data exist in a form which could provide a check on the transonic similarity law of section 3.3.

As regards the supersonic régime, few reliable experimental data have so far been published and discussion of them would perhaps better be postponed until more information has accumulated.

3.6. *The Effect of Wing Section on the Locus of Aerodynamic Centres for a Wing of Given Planform.*—In Section 2 we have observed the widely differing behaviour of the aerodynamic centre for aerofoil sections of the same family, but with different thickness ratios, and also for aerofoils of the same thickness, but of different families. It must be expected therefore, that the behaviour of the locus of aerodynamic centres of an actual three-dimensional wing will be influenced by the shape of the wing section.

Two distinct effects are involved in this connection; firstly there is the effect of the finite thickness distribution, which is present whether the flow is inviscid or viscous, and secondly there is the boundary-layer effect associated with viscous flow. In Ref. 27, Weber has presented a method of calculating the chordwise pressure distribution on the surface of a thick two-dimensional aerofoil section in potential flow, and she has extended the method to the infinite sheared wing and to the centre section of swept wings, so that in association with Küchemann's method[26], it may be used to calculate the pressure distribution over the whole surface of a thick swept wing in non-viscous flow. Since in practice, however, section thickness and viscosity effects are inseparably combined, this work will be of little help in bridging the gap between the potential flow solutions for thin aerofoils and the practical solutions for wings of finite thickness in viscous flow. At the same time, the quantity of three-dimensional experimental data which has accumulated, is quite inadequate to serve as a basis for empirical corrections for the effects in question, and we must therefore fall back on the two-dimensional data to give us an indication of the effects of wing section on the three-dimensional problem.

In order to attempt any quantitative assessment on the basis of the two-dimensional data, it is necessary to examine the velocity distribution over the wing in relation to the critical Mach numbers appertaining to three characteristic sections of the wing—the central kink section, the tip section and a section in what Neumark[28] calls the ' regular region ' of the wing (*i.e.*, a section, as a considerable distance from both the kink and the tip, where the flow approximates to that of an infinite sheared wing). Provided that the wing under consideration is of fairly large aspect ratio and moderate taper, Neumark's work* may be used to estimate roughly, for the kink and regular sections†, ranges of ' two-dimensional equivalent ' Mach numbers corresponding to a given range of free-stream Mach numbers. The effect of thickness and viscosity on the local aerodynamic centre at either characteristic section, for a given free-stream Mach number, may now be assumed to be the same as for the appropriate section in two-dimensional flow at the ' two-dimensional equivalent ' Mach number. Conditions at the tip are so dependent on the precise shape of the tip that it is hardly worth while attempting a similar analysis there, and in most practical cases it should be good enough to apply the regular region correction right out to the tip. Corrections for sections between the kink and the regular region may be obtained by judicious interpolation.

The above procedure is described in somewhat greater detail, and illustrated by a worked example in Appendix I. It should be emphasised that it represents a tentative proposal for dealing with the problem rather than an established method, and that it might need modification in the light of experience. Generally speaking, we may expect the method to be most reliable for wings of large aspect ratio; there are some indications that it may overestimate the corrections when the aspect ratio is small.

---

* Strictly applicable only to untapered wings.

† *N.B.* Sections normal to the mean direction of the isobars.

4. *Concluding Remarks.*—From the foregoing review of existing theoretical and experimental information, it will have become apparent that there are large gaps in our knowledge of the behaviour of the local aerodynamic centre of aerofoils in two and three dimensions.

Theoretical work relating to three-dimensional flow has been confined almost exclusively to thin aerofoils in inviscid flow, and there is, as yet, no established method of allowing for the Reynolds number and transition position effects, which are associated with viscous flow about aerofoils of finite thickness, and which the two-dimensional experimental data have shown to be so important.

On the experimental side there has accumulated somewhat haphazardly, a fairly large quantity of two-dimensional data, relating to the subsonic régime and to the lower end of the transonic régime ; for three-dimensional aerofoils, these regions have been very inadequately explored, particularly as regards the effect of section thickness, while both for two-dimensional and three-dimensional aerofoils, the upper parts of the transonic, and the whole of the supersonic régimes remain almost completely unknown territory.

For two-dimensional flow, existing theories completely fail to predict the large shifts of aerodynamic centre that may, in fact, occur in the subsonic régime. Except possibly for very thin aerofoils (t/c of the order 6 per cent or less) such shifts are usually in the forward direction and tend to increase with increasing thickness. Although it is evident that, as Mach number increases, the aerodynamic centre must ultimately move back towards its supersonic position near the mid-chord point, experimental data for the transonic region are such as to suggest that the mode of translation will remain unpredictable.

For three-dimensional aerofoils in the subsonic régime, potential flow theories give results which are usually in reasonably good agreement with experiment, at least qualitatively, although there appears to be a tendency for theory to predict a more pronounced forward trend of the local aerodynamic centre towards the tips of swept-back wings, than actually occurs in practice. An assessment of the two-dimensional characteristics of the wing section(s), should indicate the direction, if not the magnitude, of the corrections which should be applied to allow for the effects of finite thickness and viscosity.

In the circumstances summarised above, it is clearly impossible to give a prescription for determining exactly the behaviour of the local aerodynamic centres of a given wing in the three régimes of compressible flow. At the same time it is evident that, while it would be relatively simple to draw up a comprehensive programme of research designed to close the remaining gaps in our knowledge, such a programme would be impossible of achievement with the resources available. Lest this report should end on too pessimistic and inconclusive a note, however, we may suggest a scheme, whereby the assembled experimental data, examined against the theoretical background, may be used for an approximate assessment of aerodynamic-centre positions, and also indicate where any immediate research effort might most usefully be concentrated.

4.1. *Suggested Procedure for Estimating Local Aerodynamic Centre Positions for a Wing of Specified Plan-form and Aerofoil Section(s).*—Apart from quoting results of Puckett's and Stewart's external supersonic conical solution for wings with pointed tips (section 3.4 and Fig. 30) this report has not attempted to cover the supersonic régime, and the calculation procedure now outlined applies only to Mach numbers less than 1·0.

Procedure.—(i) Obtain the flat-plate incompressible potential flow solution for the given plan-form using one of the methods (Falkner, Multhopp, or Küchemann) discussed in this report*, and also by use of the ' equivalent wing ' concept, obtain corresponding solutions for a range of subsonic Mach numbers.

* It should be noted that the methods of Falkner and Multhopp give local aerodynamic centres based on the assumption that the two-dimensional aerodynamic centre lies at the quarter-chord, whereas Küchemann's method gives the displacements of the local aerodynamic centres from the position in two-dimensional flow.

These results need some correction to allow for the effects of finite thickness and viscosity. As suggested in section 3.6, the direction and approximate magnitude of these corrections may best be determined from two-dimensional experimental data. Thus:

(ii) *For incompressible flow :* Calculate the aerodynamic-centre position of the chordwise section(s) of the wing by Thomas's method (Ref. 2). Use this value either to correct the flat-plate solution (if obtained by Falkner's or Multhopp's method) or, in conjunction with Küchemann's method, to obtain the absolute positions of the local aerodynamic centres in viscous flow.

(iii) *For compressible flow :* For each value of M, apply the incompressible flow correction of (ii) above, to the appropriate flat-plate potential flow solution obtained as in (i). Then

(*a*) Consider two sections*, one in the kink and the other in the regular region of the wing and for each, determine in the manner described in Appendix I, the ' two-dimensional equivalent ' Mach numbers corresponding to the free-stream Mach numbers under consideration.

(*b*) For each section, use the experimental data of this report to estimate the shifts of aerodynamic centre from the incompressible flow position, at each of the appropriate ' two-dimensional equivalent ' Mach numbers, and plot the shifts against the corresponding free-stream Mach numbers. In general, it will be necessary to examine in turn the influence of

Section thickness: *see* Table 2

Position of section maximum thickness: *see* Table 3

Camber: *see* Table 4.

Apply the calculated shifts as additional corrections to the flat-plate solutions, interpolating between the values at the kink and regular sections for intermediate sections. The shape of the basic ' flat-plate ' curve should provide sufficient guide to the mode of interpolation. In view of the uncertain conditions prevailing at the wing tips, it is suggested (*see* section 3.6) that the regular region correction should be applied right out to the tip.

The above procedure has been applied in an illustrative example worked out in Appendix I; the results suggest that the method may tend to overestimate the corrections to be applied.

4.2. *Suggestions for Future Research*†.—Great interest attaches to the behaviour of local aerodynamic centres in the transonic régime, but experimental investigation must await the development of a satisfactory transonic test technique‡. Meanwhile any immediate research effort must, of necessity, relate to the subsonic or supersonic régimes, in the latter of which, progress must be handicapped by inadequate tunnel facilities.

As regards subsonic research, efforts would perhaps be most usefully directed towards correlating the theoretical (flat-plate—potential flow) methods of calculation with experimental results, and establishing a reliable method of correcting for finite thickness and viscosity. This would necessitate:

(*a*) Systematic calculations by the various methods, for families of practical wing plan-forms§.

---

* Normal to the mean direction of the isobars.

† *Footnote added* 1957.

Developments in test facilities and techniques, and changes in aircraft design philosophy which have occurred during the past seven years might suggest revision of this section in one or two respects, but broadly speaking, the recommendations still stand.

‡ The ' transonic bump ' and ' wing flow ' techniques offer perhaps the best hope for the immediate future in that they require only the adaptation of existing equipment rather than the development of essentially new apparatus.

§ Some work of this nature has already been started at the R.A.E. and at the N.P.L.

(*b*) Pressure-plotting tests, over a wide range of subsonic Mach numbers, on some or all of these plan-forms, all test wings to have the same aerofoil section, which should preferably be of a type for which the variation of aerodynamic centre with Mach number (sub-critical) is known to be small.

(*c*) Additional pressure-plotting tests on at least two of the above plan-forms (one of large, and one of small aspect ratio) associated with one or more alternative aerofoil sections which are known to exhibit large variations of aerodynamic centre with Mach number.

The limited facilities for supersonic research might be devoted to providing experimental checks on the external conical solution for pointed wings (section 3.4 and Fig. 30). A delta wing has already been pressure plotted in the R.A.E. 9-in. square Supersonic Wind Tunnel.

REFERENCES

General

No.	*Author*	*Title, etc.*
1	S. B. Gates	Notes on the transonic movement of wing aerodynamic centre. R. & M. 2785. May, 1949.
2	H. H. B. M. Thomas	Correlation of the position of the aerodynamic centre of an aerofoil with the rate of change of the lift coefficient with incidence. R.A.E. Tech. Note Aero. 2029. A.R.C. 12,965. November, 1949.
3	J. H. Preston	Correlation of the position of the aerodynamic centre with lift slope for a variety of aerofoils in various wind tunnels. A.R.C. 6809. June, 1943.
4	H. H. B. M. Thomas	Correlation of experimental and theoretical hinge moments for plain controls. R.A.E. Report Aero. 2238. A.R.C. 11,401. March, 1948.
5	L. W. Bryant	Two-dimensional control characteristics. Part I: Lift due to plain flap. A.R.C. 9534 (revised). April, 1947.
6	L. W. Bryant, A. S. Halliday and A. S. Batson.	Two-dimensional control characteristics. Part IV: Variation of pitching moments with incidence and control angle. R. & M. 2730. April, 1950.
7	R. Dickson	The relationship between the compressible flow round a swept-back aerofoil and the incompressible flow round equivalent aerofoils. R.A.E. Report Aero. 2146. A.R.C. 9986. August, 1946.
8	von Karman	Compressibility effects in aerodynamics. *J. Ae. Sci.* July, 1941. (Also A.R.C. 5314.)
9	A. D. Young	A survey of compressibility effects in aeronautics. R.A.E. Report Aero. 1725. A.R.C. 5749. February, 1942.
10	Carl Kaplan	A theoretical study of the moment on a body in a compressible fluid. N.A.C.A. Report 671. 1939.
11	J. R. Spreiter	Similarity laws for transonic flow about wings of finite span. N.A.C.A. Tech. Note 2273. A.R.C. 13,968. January, 1951.
12	W. F. Hilton	Limitations of use of Busemann's second-order supersonic aerofoil theory. R. & M. 2524. August, 1946.
13	M. J. Lighthill	Two-dimensional supersonic aerofoil theory. R. & M. 1929. January, 1944.
14	E. C. Pohmanus	Preliminary correlation of the effect of compressibility on the location of the section aerodynamic centre at subcritical speeds. N.A.C.A. Research Memo. L8D14 (TIB/2021). November, 1948.

REFERENCES—*continued*

General—continued

No.	*Author*	*Title, etc.*
15	C. M. Britland	American, German and British aerofoil notations. R.A.E. Tech. Memo. Aero. 11. January, 1948.
16	I. H. Abbott, A. E. von Doenhoff and L. S. Stivers, Jr.	Summary of airfoil data. N.A.C.A. Report 824. March, 1945.
17	H. Multhopp	Methods for calculating the lift distribution of wings (subsonic lifting-surface theory). R. & M. 2884. January, 1950
18	H. Schlichting and W. Kahlert ..	Calculation of lift distribution of swept wings. R.A.E. Report Aero. 2297. A.R.C. 12,238. October, 1948.
19	V. M. Falkner	The calculation of aerodynamic loading on surfaces of any shape. R. & M. 1910. August, 1943.
20	V. M. Falkner	The solution of lifting plane problems by vortex lattice theory. R. & M. 2591. September, 1947.
21	V. M. Falkner	Calculated loadings due to incidence of a number of straight and swept-back wings. R. & M. 2596. June, 1948.
22	H. C. Garner	Methods of approaching an accurate three-dimensional potential solution for a wing. R. & M. 2721. October, 1948.
23	H. C. Garner	Theoretical calculations of the distribution of aerodynamic loading on a delta wing. R. & M. 2819. March, 1949.
24	S. B. Berndt and K. Orlik-Rückemann.	Comparison between theoretical and experimental lift distributions of plane delta wings at low speeds and zero yaw. K.T.H. Aero. Tech. Note 10. December, 1948.
25	V. M. Falkner	A comparison of two methods of calculating wing loading with allowance for compressibility. R. & M. 2685. November, 1948.
26	D. Küchemann	A simple method for calculating the span and chordwise loadings on thin swept wings. R.A.E. Report Aero. 2392. A.R.C. 13,758. August, 1950.
27	J. Weber	A simple method for calculating the chordwise pressure distribution on two-dimensional and swept wings for aerofoil sections of finite thickness. R.A.E. Report Aero. 2391. A.R.C. 13,757. August, 1950.
28	S. Neumark	Critical Mach numbers for thin untapered swept wings at zero incidence. R. & M. 2821. November, 1949.

Experimental Data, Two-Dimensional

No.	*Author*	*Title, etc.*
E.1	W. F. Lindsey, D. B. Stevenson and B. N. Daley.	Aerodynamic characteristics of 24 N.A.C.A. 16-Series airfoils at Mach numbers between 0·3 and 0·8. N.A.C.A. Tech. Note 1546. September, 1948.
E.2	B. N. Daley	Effects of compressibility on the characteristics of five airfoils. N.A.C.A. Research Memo. L6L16 (T.I.B./1344). April, 1947.
E.3	D. J. Graham, G. E. Nitzberg and R. N. Olsen.	A systematic investigation of pressure distributions at high speeds over five representative N.A.C.A. low-drag and conventional airfoil sections. N.A.C.A. Report 832. May, 1947.
E.4	R. J. Ilk	High-speed aerodynamic characteristics of four thin N.A.C.A. 63-Series aerfoils. N.A.C.A. Research Memo. A7J23 (T.I.B./1501). December, 1947.
E.5	A. Anscombe	High-speed wind-tunnel tests on aerofoils H.S.1 and H.S.2. R.A.E. Report Aero. 1811. A.R.C. 6740. March, 1943.

REFERENCES—*continued*

Experimental Data, Two-Dimensional—continued

No.	*Author*	*Title, etc.*
E.6	J. S. Thompson, M. Markowicz, J. A. Beavan and R. G. Fowler.	Pressure distribution and wake traverses on models of *Mustang* wing section in the R.A.E. and N.P.L. high-speed tunnels. R. & M. 2551. August, 1944.
E.7	J. S. Thompson and D. Adamson ..	High-speed wind-tunnel measurements of pressure distribution on an aerofoil of NACA 23021 section. R.A.E. Report Aero 1985. A.R.C. 8350. November, 1944.
E.8	W. F. Hilton	High-speed tunnel tests of two thick aerofoils. A.R.C. 7203. November, 1943.
E.9	J. A. Beavan, G. A. M. Hyde and R. G. Fowler.	Pressure and wake measurements up to Mach number 0·85 on an EC 1250 section with 25 per cent control. R. & M. 2065. February, 1945.
E.10	B. Göthert and W. A. Mair ..	German high-speed wind-tunnel results. R.A.E. Tech. Note Aero. 1684. A.R.C. 9064. August, 1945.
E.11	W. A. Mair	German high-speed wind-tunnel tests on four aerofoils of different camber. R.A.E. Tech. Note Aero. 1685. A.R.C. 9058. September, 1945.
E.12	K. W. Mangler and H. B. Squire	D.V.L. high-speed wind-tunnel tests on NACA 00012–0·55 50. R.A.E. Tech. Note Aero. 1915. A.R.C. 11,103. August, 1947
E.13	E. P. Sutton	D.V.L. high-speed tunnel tests on an NACA 00012–0·55 30 aerofoil. (1) Pressure distribution curves. R.A.E. Tech. Note Aero. 1931. January, 1948.
E.14	R. Hills and F. N. Kirk	Summary of some recent two-dimensional aerofoil tests at high subsonic *M*. R.A.E. Tech. Note Aero. 1987. A.R.C. 12,259. February, 1949.
E.15	B. Göthert	High-speed measurements on sections of series NACA 230 with different thickness ratios. NACA 230–15. D.V.L./UM 1259/3. A.R.C. 11,059. July, 1944.
E.16	B. Göthert	(*a*) Diagrams for pressure distribution for section NACA 230–12 at high subsonic speeds. D.V.L./UM 1260/2. A.R.C. 11,539. September, 1944. (*b*) Hochgeschwindigkeitsmessungen an Profilen der Reihe NACA 230 mit verschiedenen Dickenverhältnissen. Teilbericht II: NACA 230–12. D.V.L./UM 1259/2. May, 1944.
E.17	B. Göthert	(*a*) Diagrams for pressure distribution for NACA section 230–9 at high subsonic velocities. D.V.L./UM 1260/1. A.R.C. 11,550. September, 1944. (*b*) Hochgeschwindigkeitsmessungen an Profilen der Reihe NACA 230 mit verschiedenen Dickenverhältnissen. Teilbericht I: NACA 230–9. D.V.L./UM 1259/1. May, 1944.
E.18	B. Göthert	(*a*) Aerofoil measurements in the D.V.L. (2·7m) high-speed wind tunnel. D.V.L./FB 1490. N.R.C.C. Tech. Translation No. TT–31. October, 1941. (*b*) High-speed tests on symmetrical profiles with different thickness ratios in the D.V.L. high-speed wind tunnel (2·7m diam.) and comparison with measurements in other wind tunnels. N.R.C.C. Tech. Translation No. TT–38. D.V.L./FB 1506. December, 1941.
E.19	J. Stack and A. E. von Doenhoff ..	Tests of 16 related airfoils at high speeds. N.A.C.A. Report 492. 1934.
E.20	Ferri	Completed tabulation in the United States of tests of 24 airfoils at high Mach numbers. N.A.C.A. A.C.R. L5E21 (T.I.B./951). June, 1945.

REFERENCES—*continued*

Experimental Data, Three-Dimensional

No.	*Author*	*Title, etc.*
E.21	J. Weber and G. G. Brebner ..	Low-speed tests on 45-deg swept-back wings. Part I: Pressure measurements on wings of aspect ratio 5. R. & M. 2882. May, 1950.
E.22	J. Weber	Low-speed measurements of the pressure distributions and overall forces on wings of small aspect ratio and 53-deg sweepback. R.A.E. Tech Note Aero. 2017. A.R.C. 12,878. September, 1949.
E.23	O. Holme	Comparative wind-tunnel tests of a swept-back and a straight wing having equal aspect ratios. F.F.A. Report 31 (T.I.B./P 21665). 1950.
E.24	D. J. Raney..	Low-speed wind-tunnel investigation of the pressure distribution over a delta wing of aspect ratio 3·0 at small incidences. R.A.E. Tech. Note Aero. 2062. A.R.C. 13,657. July, 1950.
E.25	B. H. Wick	Chordwise and spanwise loadings measured at low speed on a triangular wing having an aspect ratio of two and an NACA 0012 airfoil section. N.A.C.A. Tech. Note 1650. June, 1948.
E.26	M. Ingelmann-Sundberg	Experimental determination of pressure distribution on a plane wing with 40 deg sweepback at low speed. K.T.H. Aero. Tech. Note 8. November, 1947.
E.27	Tunnel staff of Aero Dept. ..	Low-speed pressure distributions on a 59-deg swept wing, and comparison with high-speed results on a 45-deg swept wing. C.P. 86. February, 1949.
E.28	A. C. S. Pindar and J. R. Collingbourne.	Pressure-plotting and balance measurements in the high-speed tunnel on a half model of a 90-deg-apex delta wing with fuselage. R. & M. 2844. September, 1949.
E.29	M. Cooper and P. F. Korycinski ..	The effects of compressibility on the lift, pressure, and load characteristics of a tapered wing of NACA 66-Series airfoil sections. N.A.C.A. Tech. Note 1697. October, 1948.
E.30	R. T. Whitcomb	An investigation of the effects of sweep on the characteristics of a high-aspect-ratio wing in the Langley 8-foot high-speed tunnel. N.A.C.A. Research Memo. L6J01a (T.I.B./1116.). February, 1947.

APPENDIX I

Application of Two-dimensional Experimental Data to Determine the Effect of Finite Thickness and Viscosity on the Aerodynamic Centres of Wings of Finite Aspect Ratio

1. *General Technique.*—The following treatment is intended to apply only to wings of fairly large aspect ratio and moderate taper. Following Neumark's method[28] of dealing with critical Mach numbers for swept wings, we may consider the wing to consist of a central kink region, a tip region and an intermediate 'regular' region where the flow may be considered identical with that on an infinite sheared wing of the same profile and sweep angle. Behaviour in the tip region is so dependent upon the precise shape of the tip as to make detailed analysis of this region hardly worth while, and for our purpose, we shall assume that any corrections derived for the regular region apply right out to the tip. We are therefore reduced to considering two characteristic sections of the wing:

(i) A section in the regular region

(ii) The central kink section.

In view of the approximate nature of this investigation, we ignore the effects of the (moderate) wing taper, and measure the angle of sweepback ϕ at the quarter-chord; we further assume that the isobars in the regular region are swept back at the angle ϕ. For each characteristic section we now assume that the combined effect of thickness and viscosity at a given free-stream Mach number M_0 is the same as for the given section in two-dimensional flow at a certain equivalent Mach number M_e, which we now determine.

2. *'Two-dimensional Equivalent' Mach Numbers for the Regular Section.*—It is clear from Neumark's work (Ref. 28, sections 2 and 3) that if the wing has a chordwise section of thickness/chord ratio ϑ, and we are concerned with a free-stream Mach number M_0, then we have in effect, to consider a section with thickness ratio $\vartheta \sec \phi$ at a 'two-dimensional equivalent' Mach number $M_e = M_0 \cos \phi$.

3. *'Two-dimensional Equivalent' Mach Numbers for the Kink Section.*—For the kink section, we shall define the 'two-dimensional equivalent' Mach number corresponding to a free-stream Mach number M_0, as the free-stream Mach number M_e such that, in two-dimensional flow around the given profile at Mach number M_e, the maximum local Mach number is the same as the maximum local Mach number for the kink section in three-dimensional flow at Mach number M_0. It follows from this definition that the 'two-dimensional equivalent' of the critical Mach number for the kink section is itself critical for the two-dimensional case.

Employing Neumark's notation, we have that the maximum velocity in the kink section of a wing of sweepback ϕ in compressible flow at speed $U = M_0 a_0$ is

$$V_{\max} = M_0 a_0 \left(1 + \frac{\vartheta H'}{\sqrt{(1 - M_0^2)}}\right)$$

where H' is the value of H (the maximum super-velocity ratio per unit thickness ratio) corresponding to the angle of sweep ϕ' of the 'analogous' (Göthert) wing in incompressible flow [$\tan \phi' = \tan \phi \sqrt{(1 - M_0^2)}$]. Values of H as functions of ϕ for various aerofoil sections have been tabulated by Neumark in Ref. 28.

The local speed of sound (a) corresponding to $V_{\max}$ is given by

$$\frac{\gamma - 1}{2} M_0^2 a_0^2 + a_0^2 = \frac{\gamma - 1}{2} V_{\max}^2 + a^2$$

$$= \frac{\gamma - 1}{2} M_0^2 a_0^2 \left[1 + \frac{\vartheta H'}{\sqrt{(1 - M_0^2)}}\right]^2 + a^2$$

or

$$a^2 = a_0^2 \left\{1 - \frac{\gamma - 1}{2} M_0^2 \left(\frac{2\vartheta H'}{\sqrt{(1 - M_0^2)}} + \frac{\vartheta^2 H'^2}{1 - M_0^2}\right)\right\}.$$

The local Mach number is therefore

$$M_{\max} = \frac{V_{\max}}{a} = M_0 \frac{1 + \dfrac{\vartheta H'}{\sqrt{(1 - M_0^2)}}}{\left[1 - \dfrac{\gamma - 1}{2} M_0^2 \left(\dfrac{2\vartheta H'}{\sqrt{(1 - M_0^2)}} + \dfrac{\vartheta^2 H'^2}{1 - M_0^2}\right)\right]^{1/2}}$$

$$= M(\phi)$$

since H' is a function of ϕ.

The corresponding local Mach number in two-dimensional flow would be

$$M'_{\max} = M(0) = M_0 \frac{1 + \dfrac{\vartheta \mathrm{H}(0)}{\sqrt{(1 - M_0^2)}}}{\left[1 - \dfrac{\gamma - 1}{2} M_0^2 \left(\dfrac{2\vartheta H(0)}{\sqrt{(1 - M_0^2)}} + \dfrac{\vartheta^2 \{H(0)\}^2}{1 - M_0^2} \right) \right]^{1/2}}$$

If we plot $M_{\max}$ and $M'_{\max}$ as functions of M_0, as in Fig. 43a, and join the two curves by a horizontal line, the abscissae of its end-points A, B give one pair of corresponding values of M_0 and M_e, the ' two-dimensional equivalent ' Mach number as defined above. This process yields a curve of M_e against M_0 as in Fig. 43b.

4. *Illustrative Example.*—The tapered swept-back wing ($A = 5 \cdot 87$, $\phi_{c/4} = 45$ deg) for which experimental results are given in Fig. 40, has been used for this example. The aerofoil section was HS6 scaled up to 14 per cent thick (at 31 per cent c), the trailing-edge angle τ being about 14 deg. The aerodynamic centre of this section in incompressible flow at the test Reynolds number of $1 \cdot 5 \times 10^6$ has been estimated by Thomas's method (Ref. 2) to lie at $0 \cdot 235c$. Using this result in conjunction with Küchemann's method (Ref. 26), the loci of aerodynamic centres were calculated for $M = 0 \cdot 6$, $0 \cdot 8$ and $0 \cdot 872$, using the equivalent wing concept, and ignoring the variation of thickness and viscosity effect with M. The results are shown in Fig. 44 (broken lines), together with experimental points* from Fig. 40.

To correct for thickness and viscosity, the variation of ' two-dimensional equivalent ' Mach numbers with free-stream Mach number, for the regular and kink sections was computed in the manner indicated in sections 2 and 3 above (*see* Figs. 43a and 43b). These equivalent Mach numbers were then used, in conjunction with Fig. 4 (employing interpolation with respect to τ rather than t/c), to derive the corrections to aerodynamic-centre position for thickness and viscosity, which are shown in Fig. 43c. These corrections were now applied to the uncorrected results of Fig. 44, a rough interpolation being made between the kink and regular section results, for intermediate sections; the corrected loci are shown by the full lines of the figure.

Discussion.—Apart from the two points in mid-semispan at $M = 0 \cdot 6$, the corrections appear to be of correct sign, but except near the tip, they are too large to give agreement with the experimental results. It is not possible to draw general conclusions from this single example, but it is suspected that the proposed method of correction, based on two-dimensional data, will result in over-correction, particularly at the lower aspect ratios.

From Fig. 43c, it will be noted that at $M \simeq 0 \cdot 87$, there is a reversal of the forward-moving tendency of the kink-section aerodynamic centre due to thickness and viscosity effects, which for $M > 0 \cdot 87$, cause a rapid rearward movement; meanwhile the regular-section aerodynamic centre continues to move forward due to these effects. At these high Mach numbers, for which the local flow is already supersonic over parts of the wing, it is no longer permissible to apply the ' equivalent wing ' concept in assessing the effect of plan-form, but assuming that this effect suffers no sudden change at $M \simeq 0 \cdot 87$, it may be concluded that above this Mach number, the kink-section aerodynamic section should move rapidly rearward, while in the regular section, the aerodynamic centre should, if anything, move slightly forward. This agrees roughly with the observed experimental behaviour, as evidenced by the curves of Fig. 40 for $M = 0 \cdot 893$ and $0 \cdot 915$. It thus appears that two-dimensional data, applied in the manner suggested in this appendix, should give a reasonable qualitative indication of behaviour at the lower end of the transonic régime.

---

* Note that the experimental points are actually centres of pressure, not aerodynamic centres. Since the aerofoil section is symmetrical, however, there should, by linear theory, be no difference.

TABLE 1—*Sources of*

Item No.	Report No.	Ref. No.	Aerofoil section(s)	Type of section and remarks	t/c (per cent)	Position of $(t/c)_{max}$ (% chord)	Camber (per cent)	Trailing edge
1	N.A.C.A./ T.N.1546	E.1	24 NACA 16 Series	High-speed sections (particularly for propeller applications). Various amounts of camber	6 to 30	50	0 to 5·52	Convex
2	N.A.C.A./ T.I.B./1344	E.2	NACA:					
			23015	Older conventional	15	30	1·84	Convex
			16–212	High critical speed	12	50	1·10	Convex
			66, 2–015	Low-drag	15	45	0	Concave
			66, 2–215		15	45	1·10	
			65 (216)–418		18	40	2·21	
3	N.A.C.A./ T.I.B./1365	E.3	NACA:					
			0015	Conventional symmetric ..	15	30	0	Convex
			4415	Highly positive cambered conventional.	15	30	4	Convex
			23015	Forward cambered conventional	15	30	1·84	Convex
			65_2–215	Low-drag	15	40	1·50	Concave
			66, 2–215		15	45	1·48	Concave
4	N.A.C.A./ T.I.B./1501	E.4	NACA:					
			63–206	Sections having uniform load type mean camber line (design $C_L = 0·2$).	6	35	1·10	Concave
			63–208		8	35	1·10	
			63–210		10	35	1·10	
			63–212		12	35	1·10	
5	R.A.E. Report Aero. 1811	E.5	H.S.1	Designed for high M_{crit} with satisfactory $C_{L\,max}$.	15	40·6	≃1·0	Concave
			H.S.2		12	40·6	≃1·0	
6	R.A.E. Report Aero. 1948	E.6	*Mustang* wing section	Low-drag (Models copied from templates of full-scale wing).	14·5	40	1·2	Concave
7	R.A.E. Report Aero. 1985	E.7	N.A.C.A. 23021	Older conventional	21	30	1·84	Convex
8	A.R.C. 7203	E.8	RAF 69	Thick, moderately cambered ..	20·7		1·9	Convex
			RAE 89		25		1·9	
9	A.R.C. 8395	E.9	EC. 1250 (with 25 per cent control).	Low-drag. Very similar to NACA 00012–0·55 50 (*see* Item No. 12).	12	50	0	Convex
10	R.A.E. Tech. Note Aero. 1684	E.10	NACA 0 0012–0·55 50 with various T.E. shapes.	Symmetrical; T.E. angles $\tau =$ 31·2 deg, 17·1 deg, 6·8 deg	12	50	0	Convex / Concave

Two-Dimensional Experimental Data

Trailing edge angle τ (deg)	Type of measurement	Mach number range	Reynolds number range	Method of presentation of results in reference report	Results given in this report	Figure No.
14·7 (6%) 48·7 (21%)	Force measurements	0·3 to 0·8	$0{\cdot}85 \times 10^6$ to 2×10^6	$C_{m\,c/4}$ vs. C_L curves at various M.	(i) Effect of t/c on variation of a.c. with M. (ii) Effect of camber on variation of a.c. with M.	7 16 and 17
19·5 29 12·85 12·85 8·8	Pressure distribution	0·34 to 0·75	$0{\cdot}7 \times 10^6$ to $1{\cdot}8 \times 10^6$	$C_{m\,c/4}$ and C_n curves at various M (obtained by integration). Curves of $\partial C_{m\,c/4}/\partial C_n$ vs. M are given.	Variation of a.c. with M (low C_L).	21a
19·5 19·5 19·5 9·8 12·85	Force measurements Pressure distribution	0·3 to 0·85	10^6 to 2×10^6	$C_{m\,c/4}$ vs. C_L curves at various M.	Variation of a.c. with M. $(0 \leqslant C_L \leqslant 0{\cdot}4)$	21b
3·2 4·1 4·9 5·7	Force measurements	0·3 to 0·875	10^6 to 2×10^6	$C_{m\,c/4}$ vs. C_L curves at various M.	Effect of t/c on variation of a.c. with M.	10
7·6 6·2	Force measurements	0·2 to 0·8	$0{\cdot}97 \times 10^6$ to $1{\cdot}11 \times 10^6$ $0{\cdot}83 \times 10^6$ to $1{\cdot}10 \times 10^6$	$C_{m\,c/4}$ vs. C_L curves at various M. Mean values of dC_m/dC_L for $C_L = 0$ to 0·2 are tabulated.	Variation of a.c. with M.	9
7·3	Pressure distribution	R.A.E. tests: 0·3 to 0·8 N.P.L. tests: 0·3 to 0·83	$\doteq 2 \times 10^6$ $1{\cdot}1 \times 10^6$ at $M = 0{\cdot}4$ $1{\cdot}8 \times 10^6$ at $M = 0{\cdot}8$	C_L, C_m carpets for R.A.E. tests. C_L carpet and C_m vs. M curves at various α for N.P.L. tests.	Comparative curves of a.c. variation with M (R.A.E. and N.P.L. tests).	18
24	Pressure distribution	0·4 to 0·75	2×10^6	C_L carpet, and C_m vs. M curves for various α.	Variation of a.c. with M (compared with 9%, 12% and 15% sections).	5
—	Force measurements	0·45 to 0·80	—	C_L carpet, and C_m vs. α curves for various M.	Variation of a.c. with M.	8
30	Pressure distribution, integrated to give lift and pitching moment	0·3 to 0·85	$-1{\cdot}9 \times 10^6$	Curves: C_L vs. M, C_m vs. M for various α. C_L vs. α, C_m vs. α for various M	Curves of variation of a.c. and $\partial C_L/\partial\alpha$ with M, compared with corresponding curves for Item 12	19 20
31·2 17·1 6·8	—	$M = 0{\cdot}5$	—	$C_{m\,c/4}$ vs. C_L curves	$C_{m\,c/4}$ vs. C_L curves and derived a.c. positions	14

TABLE 1

Item No.	Report No.	Ref. No.	Aerofoil section(s)	Type of section and remarks	t/c (per cent)	Position of $(t/c)_{max}$ (% chord)	Camber (per cent)	Trailing edge
11	R.A.E. Tech. Note Aero.1685	E.11	NACA: 0 0012–0·55 40 1 3512–0·55 40 2 3512–0·55 40 4 3512–0·55 40	Symmetrical; $(t/c)_{max}$ at 40%c 1% camber at 35%c 2% camber at 35%c 4% camber at 35%c	12	40 40 40 40	0 1 2 4	Convex
12	R.A.E. Tech. Note Aero. 1915	E.12	NACA: 0 0012–0·55 50	Symmetrical; $(t/c)_{max}$ at 50%c very similar to EC. 1250 (*see* Item No. 9).	12	50	0	Convex
13	R.A.E. Tech. Note Aero. 1931	E.13	NACA: 0 0012–0·55 30	Symmetrical; $(t/c)_{max}$ at 30%c	12	30	0	Convex
14	R.A.E. Tech. Note Aero. 1987	E.14	NACA: 0 0012–0·55 30 0 0012–0·55 40 0 0012–0·55 50	Symmetrical; $(t/c)_{max}$ at 30%c 40%c 50%c	12	30 40 50	0 0 0	Convex
15	A.R.C. 11059 (D.V.L./U.M. 1259/3)	E.15	NACA 23015	Older conventional	15	30	1·84	Convex
16(*a*) (*b*)	A.R.C. 11,539 and D.V.L./U.M. 1259/2	E.16	NACA 23012	Older conventional ..	12	30	1·84	Convex
17(*a*) (*b*)	A.R.C. 11,550 and D.V.L./U.M. 1259/1	E.17	NACA 23009	Older conventional	9	30	1·84	Convex
18(*a*) (*b*)	D.V.L. F.B. 1490 D.V.L. F.B. 1506	E.18	NACA: 0 00 06–1·1 30 0 00 09–1·1 30 0 00 12–1·1 30 0 00 15–1·1 30 0 00 18–1·1 30	Symmetrical with $(t/c)_{max}$ at 30 per cent chord	6 9 12 15 18	30	0	Convex
								Reports used by Polhamus in the
19	N.A.C.A. Report 492	E.19	NACA 13 Related symmetrical, and 3 cambered.	Various	6 9 12	Various (20 to 60)	0 2 4	Convex
20	N.A.C.A. T.I.B./951	E.20	24 sections mostly NACA symmetrical and cambered.	Various	4 to 15	Various (30 to 40)	Various	Convex

-continued

Trailing edge angle τ (deg)	Type of measurement	Mach number range	Reynolds number range	Method of presentation of results in reference report	Results given in this report	Figure No.
20·9	Pressure distribution	0·3 to 0·85	$2·3 \times 10^6$ to $4·6 \times 10^6$	Curves of $d/C_{m\,c/4}/dC_L$ vs. M at two C_L's	Effect of camber on variation of a.c. with M	15
30	Pressure distribution	0·3 to 0·87	$3·4 \times 10^6$ to $6·5 \times 10^6$	Curves of $d/C_{m\,c/4}/dC_L$ vs. M for various C_L	*See* Item 9	19 20
15·8	Pressure distribution	0·29 to 0·79	$2·3 \times 10^6$ to $6·2 \times 10^6$	Pressure distribution curves only are given	—	—
15·8 20·9 30	Pressure distribution	0·4 to 0·865	—	$C_{m\,c/4}$ vs. C_L curves for various M	Effect of position of $(t/c)_{max}$ on variation of a.c. with M	12
19·6	Pressure distribution	0·3 to 0·87	$2·1 \times 10^6$ to $4·5 \times 10^6$	Curves of $\partial C_{m\,c/4}/\partial C_L$ vs. M for various C_L	Effect of t/c on variation of a.c. with M (in conjunction with items 16 and 17)	5
15·6	Pressure distribution	0·29 to 0·88	2×10^6 to $4·6 \times 10^6$	Pressure distribution curves only are given	*See* item 15	5
11·7	Pressure distribution	0·29 to 0·88	$2·15 \times 10^6$ to $4·6 \times 10^6$	Pressure distribution curves only are given	*See* item 15	5
8 11·9 15·7 19·5 23·5	Pressure distribution	0·3 to 0·88 0·3 to 0·866 0·3 to 0·84 0·3 to 0·84 0·3 to 0·809	$3·2 \times 10^6$ to $6·5 \times 10^6$ (approx.)	Curves of $\partial C_{m\,c/4}/\partial C_L$ vs. M for $C_L = 0$	(i) Position of a.c. as function of M (ii) $\partial C_L/\partial \alpha_\infty$ vs. M (iii) Shift of a.c. relative to position in incompressible flow	2 3 4
correlation of Ref. 14 (*in addition to* 1 *above*)						
Various	Force measurements	0·35 to 0·87	$0·35 \times 10^6$ to $0·75 \times 10^6$	$C_{m\,c/4}$ vs. C_L curves for various M	(i) Polhamus' correlation (ii) Effect of position of $(t/c)_{max}$ on variation of a.c. with M	1 13
Various	Force measurements	0·65 to 0·94	$0·34 \times 10^6$ to $0·42 \times 10^6$	$C_{m\,c/4}$ vs. C_L curves for various M	Polhamus' correlation	1

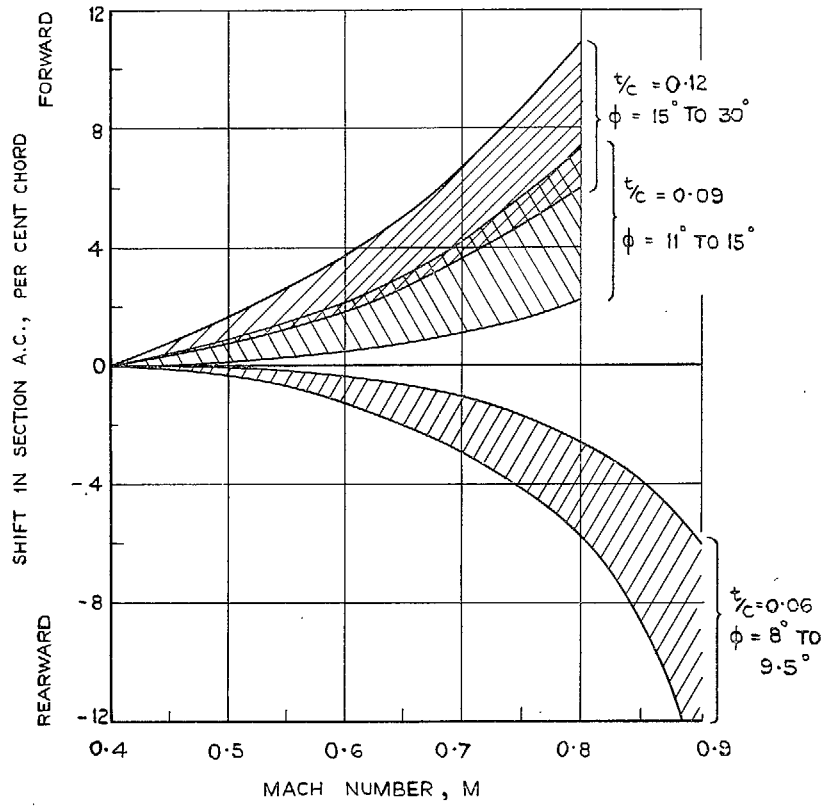

FIG. 1. Effect of Mach number on the location of the section aerodynamic centre at low lift-coefficients according to Polhamus. (Ref. 14.)

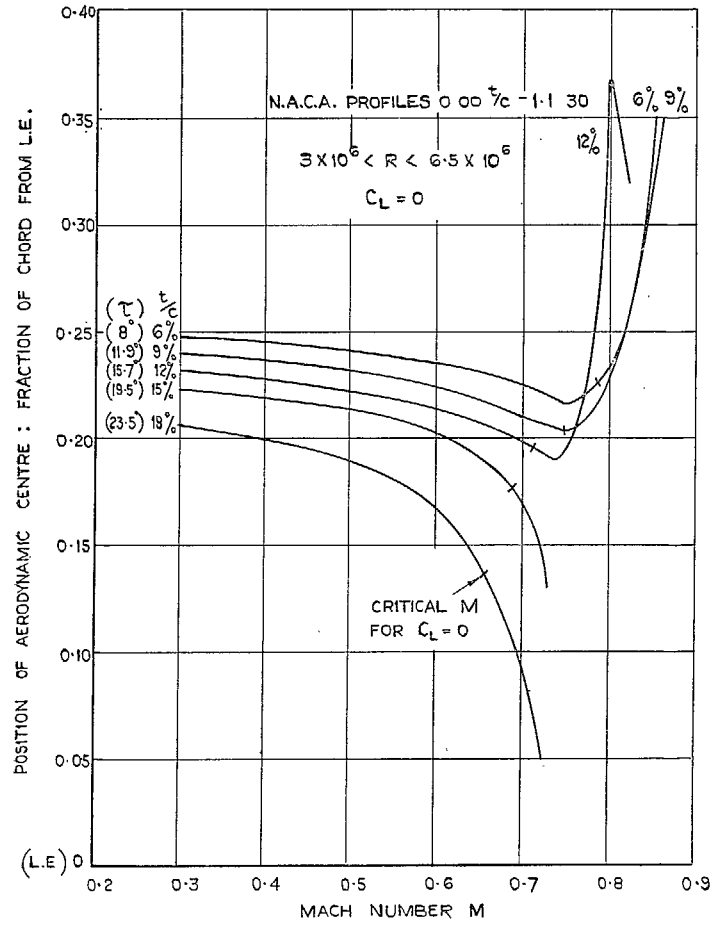

FIG. 2. Effect of t/c on variation of aerodynamic-centre position with M : N.A.C.A. Symmetrical aerofoils.

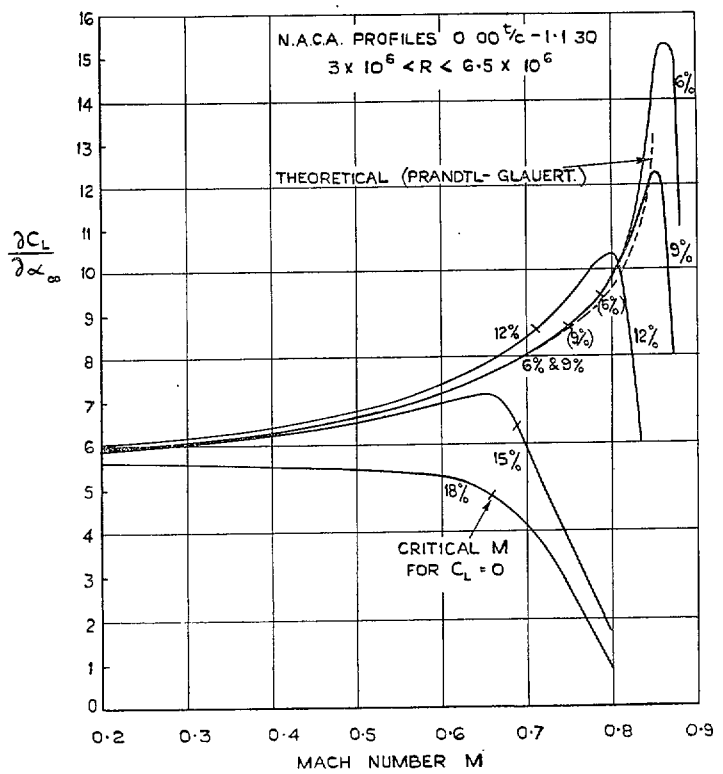

FIG. 3. Variation of lift slope with M for N.A.C.A. symmetrical aerofoils.

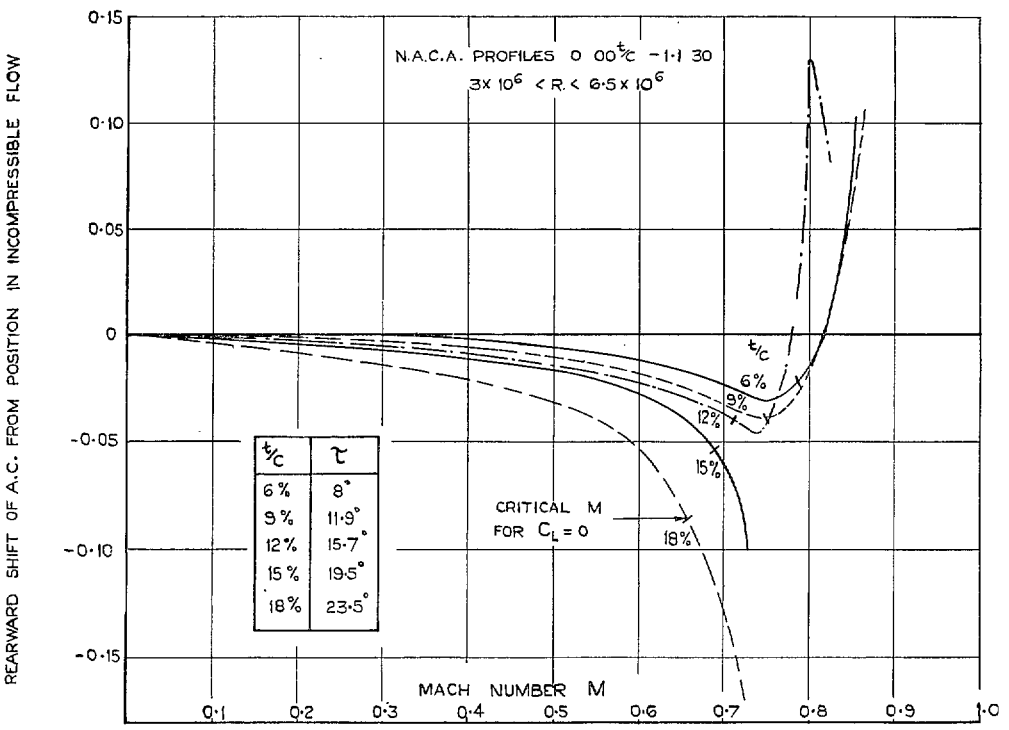

FIG. 4. N.A.C.A. symmetrical aerofoils : variation of aerodynamic-centre position from position in incompressible flow.

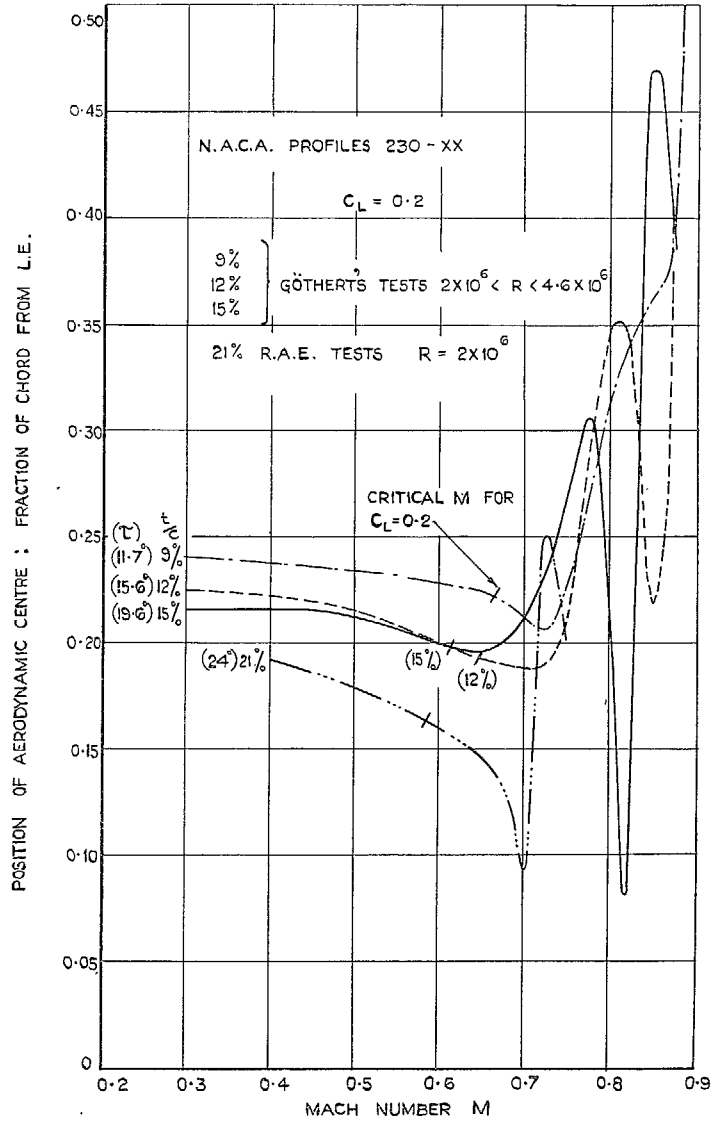

FIG. 5. Effect of t/c on variation of aerodynamic-centre position with M: N.A.C.A. cambered aerofoils

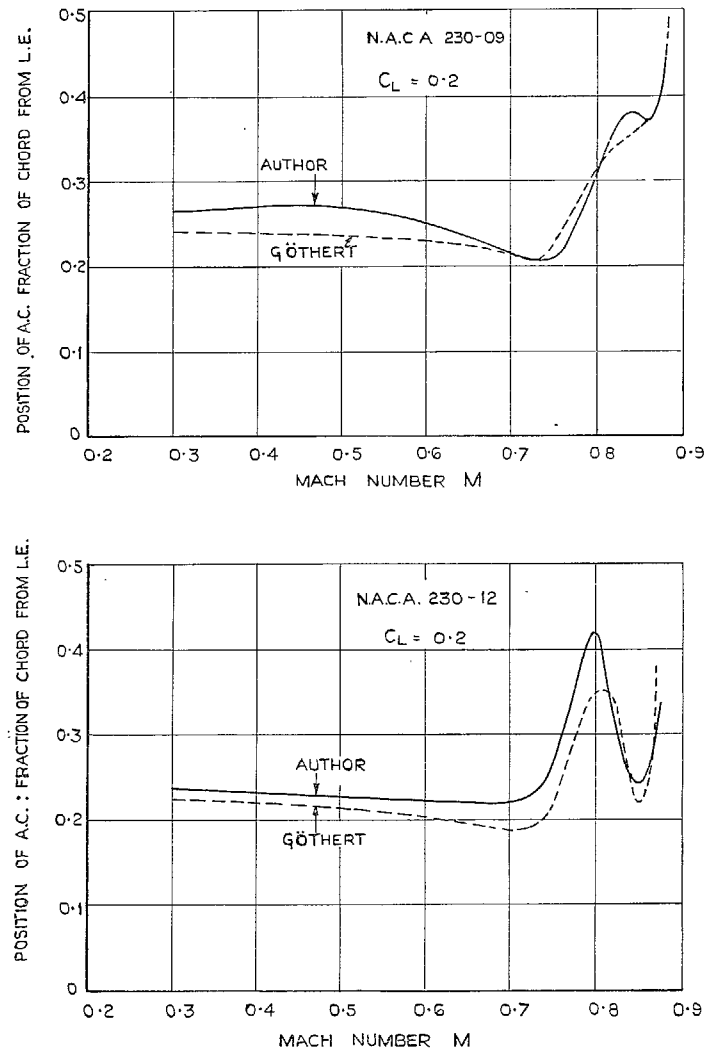

FIG. 6. Comparison of independent estimates of aerodynamic-centre position based on the same pressure distribution measurements.

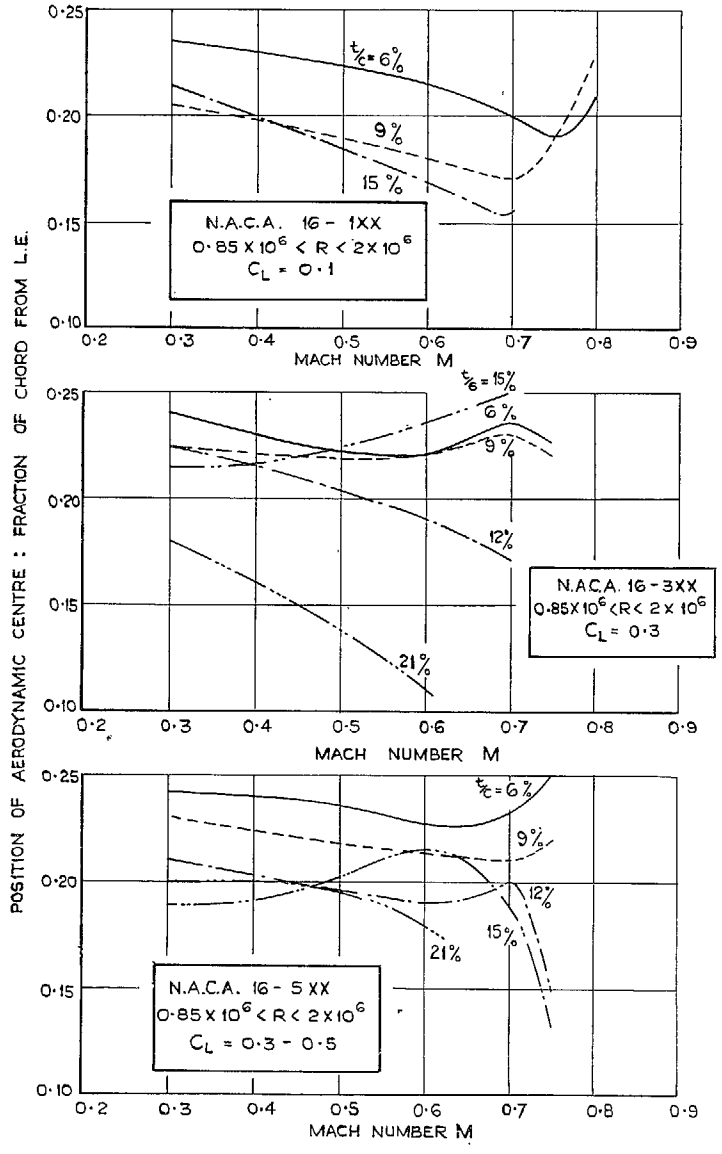

FIG. 7. Effect of t/c on variation of aerodynamic-centre position with M: NACA 16 series aerofoils.

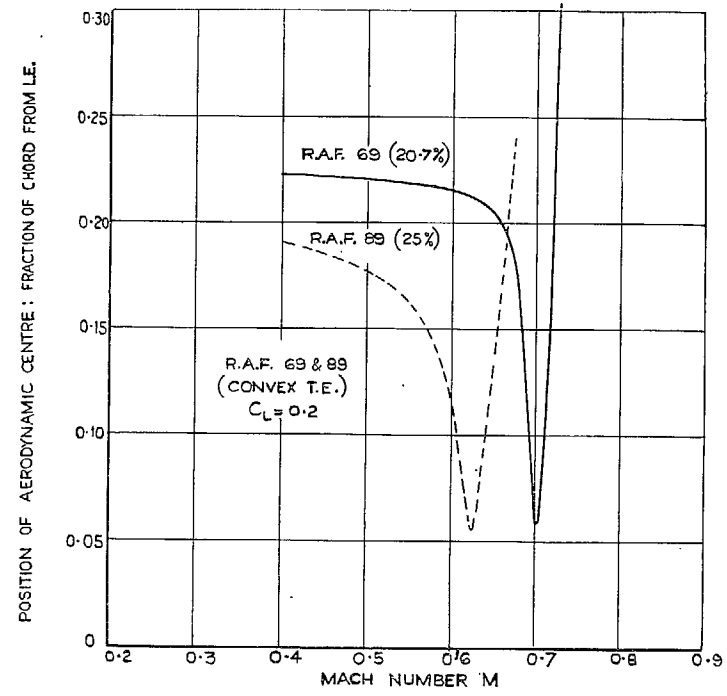

FIG. 8. Variation of aerodynamic centre for two thick aerofoils. (RAF 69 and 89.)

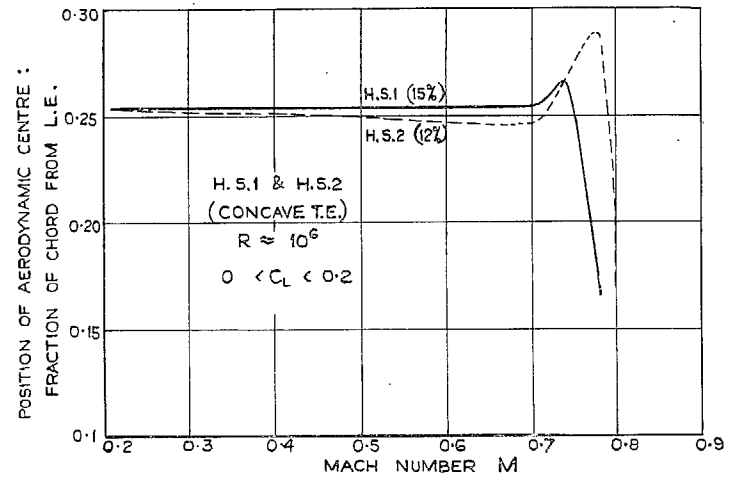

FIG. 9. Variation of aerodynamic centre for two high-speed aerofoils. (H.S.1 and H.S.2.)

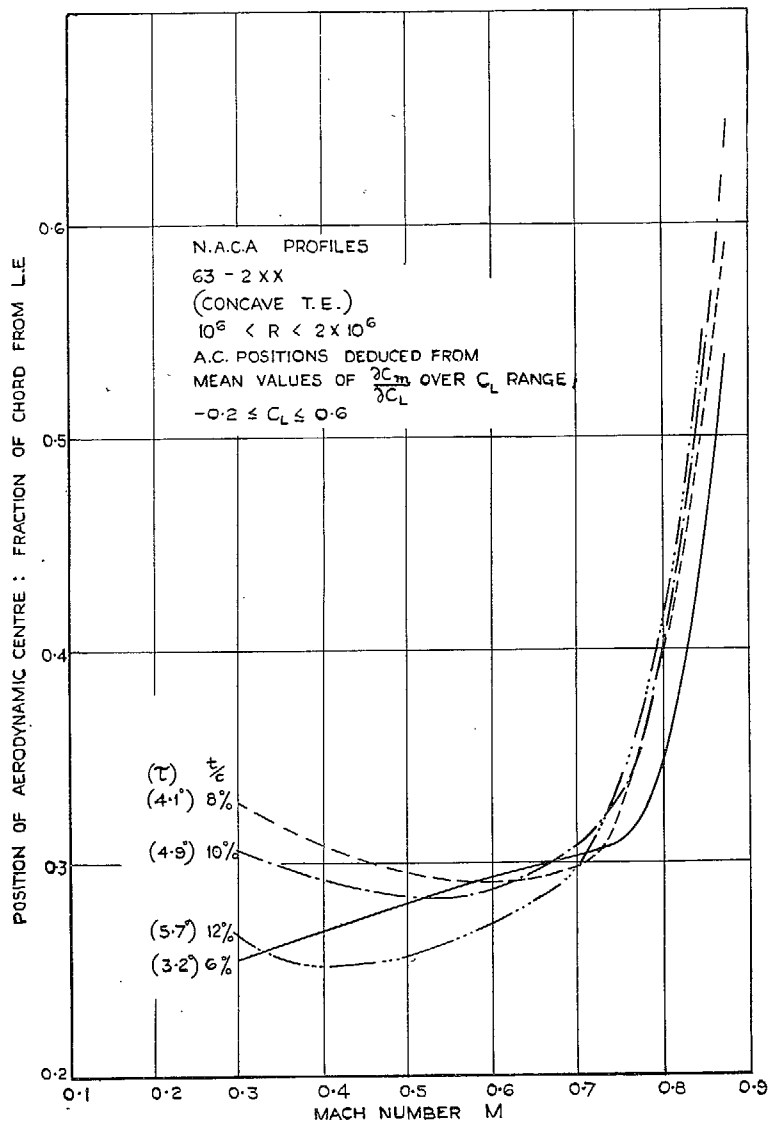

FIG. 10. Effect of t/c on variation of aerodynamic-centre position with M. NACA 63 series aerofoils.

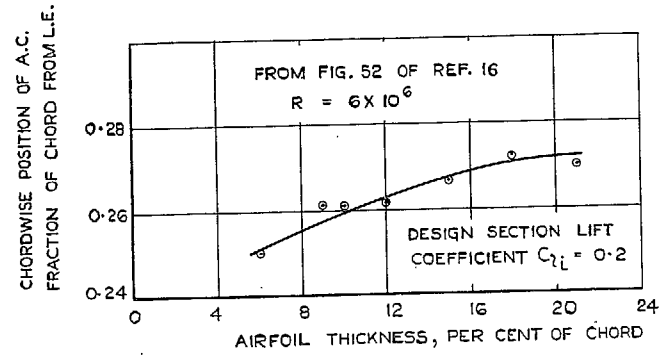

FIG 11. Variation of aerodynamic-centre position with t/c for 63–2XX aerofoils, from low-speed tests.

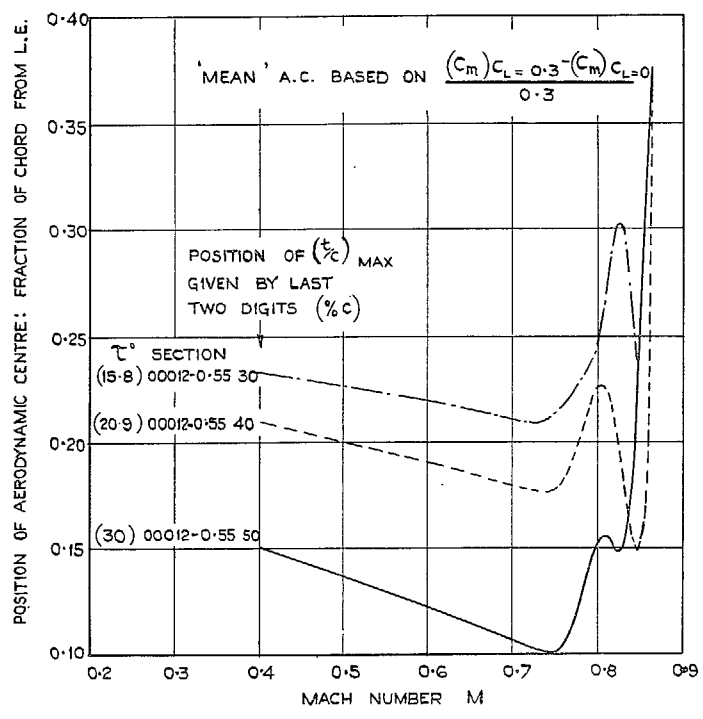

FIG. 12. Effect of position of maximum thickness on variation of aerodynamic-centre position with Mach number.
N.A.C.A. symmetrical aerofoils. $t/c = 12$ per cent.

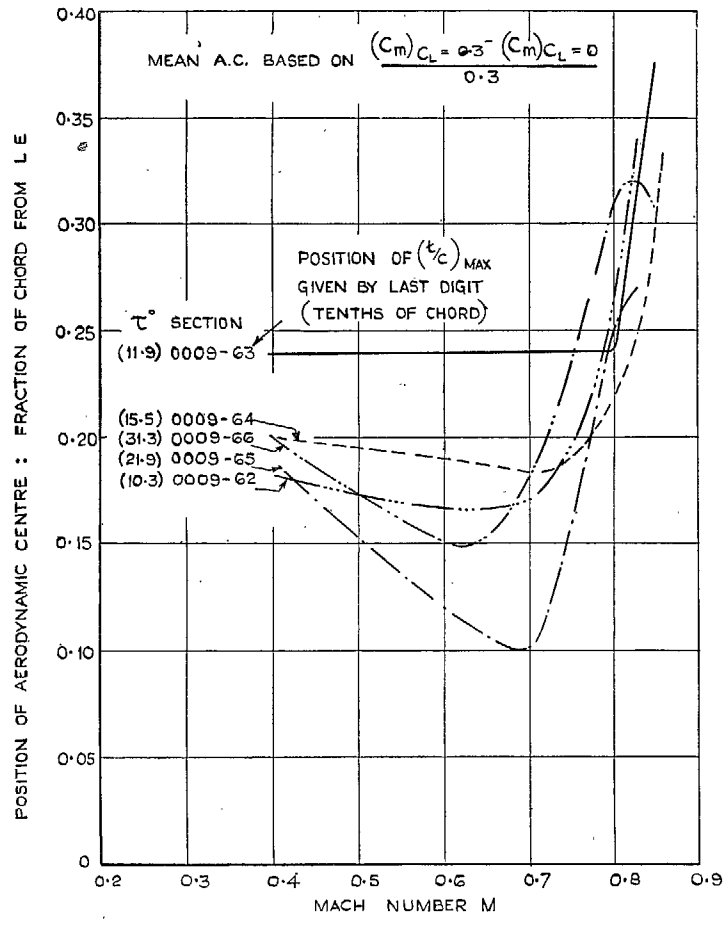

FIG. 13. Effect of position of maximum thickness on variation of aerodynamic-centre position with Mach number.

N.A.C.A. symmetrical aerofoils. $t/c = 9$ per cent.

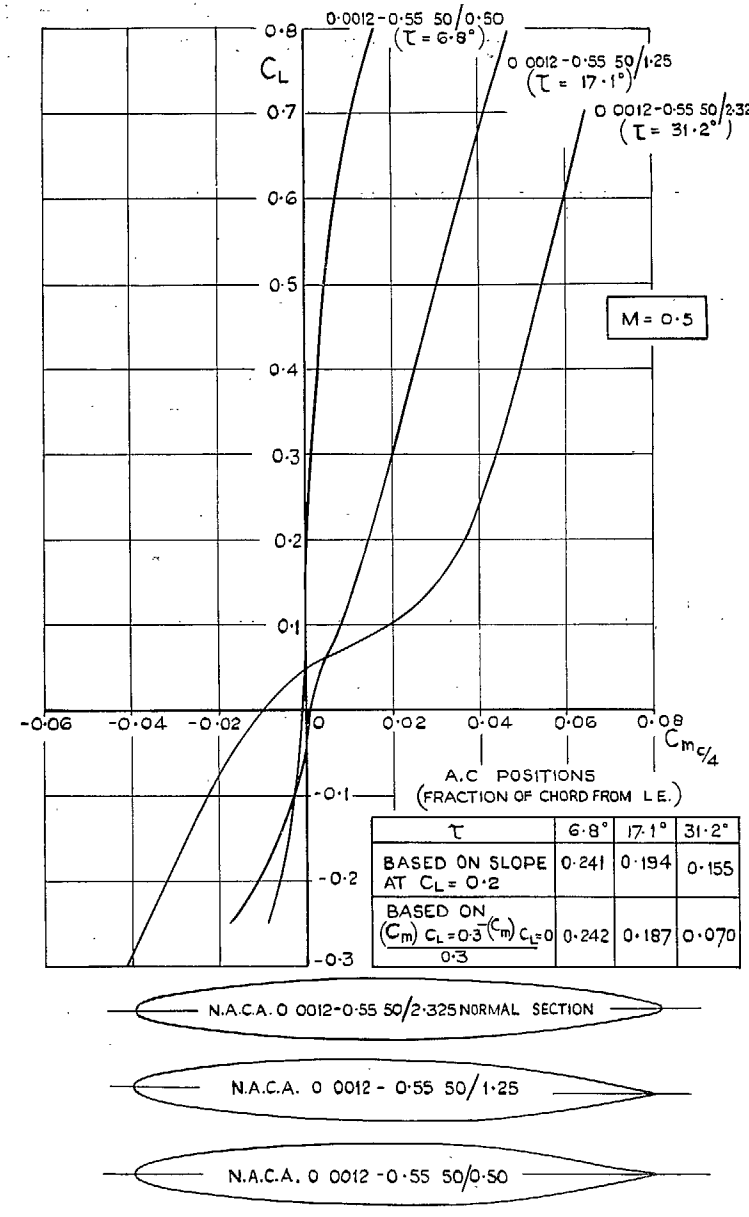

τ	6·8°	17·1°	31·2°
BASED ON SLOPE AT $C_L = 0·2$	0·241	0·194	0·155
BASED ON $\frac{(C_m)_{C_L=0·3} - (C_m)_{C_L=0}}{0·3}$	0·242	0·187	0·070

FIG. 14. Effect of trailing-edge angle on pitching-moment curves and aerodynamic centre.

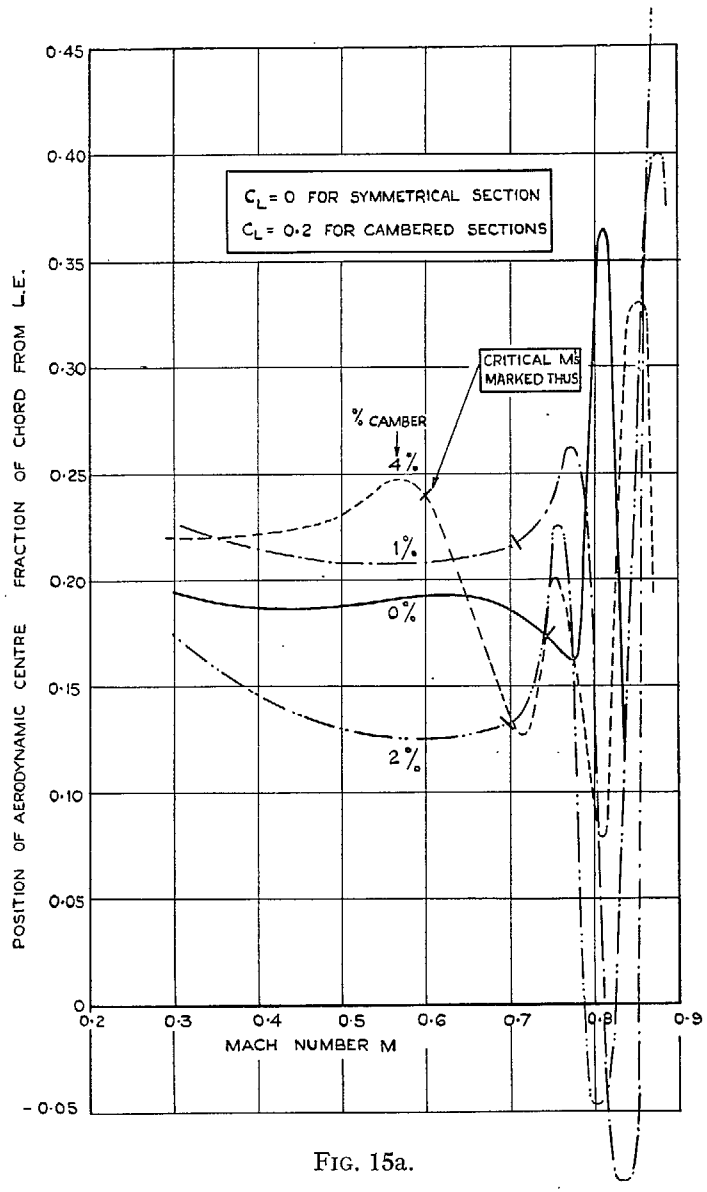

FIG. 15a.

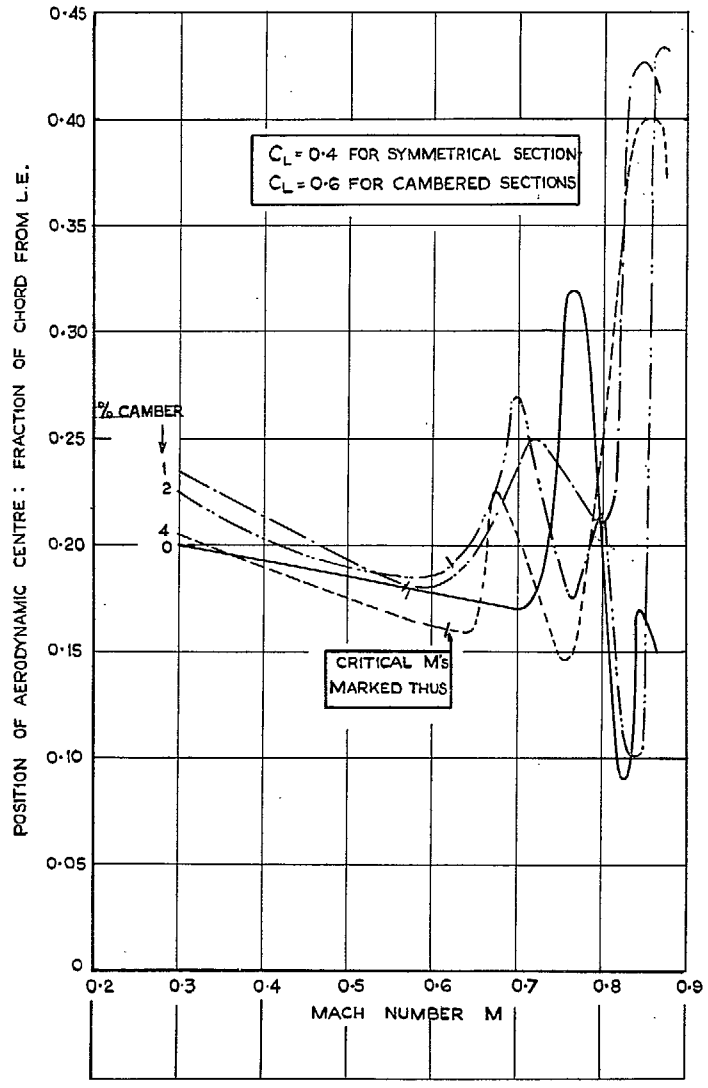

FIG. 15b.

FIGS. 15a and 15b. Effect of camber on variation of aerodynamic-centre position with M.
N.A.C.A. sections with $t/c = 0{\cdot}12$ at $0{\cdot}40c$.

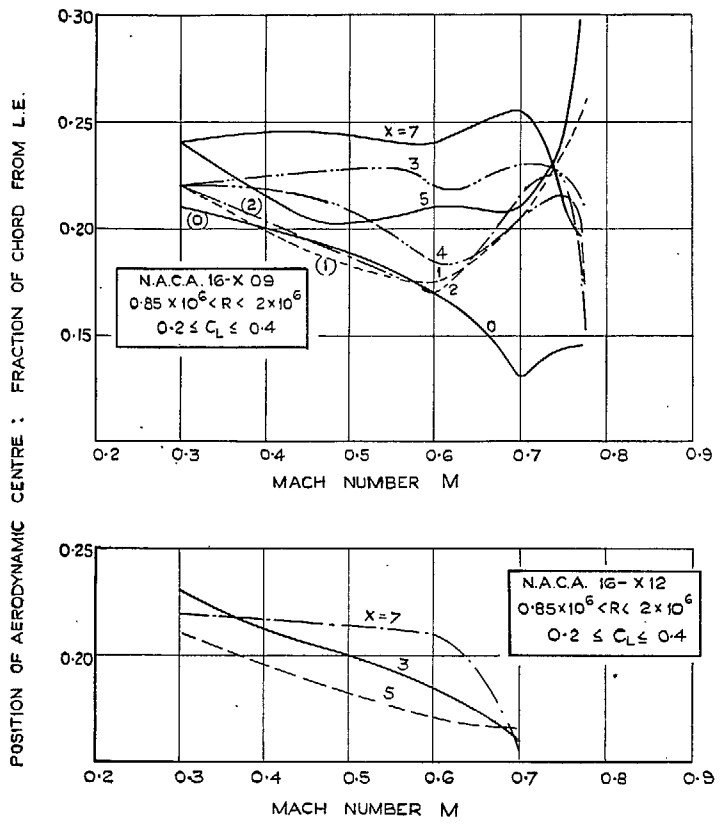

X = DESIGN C_L IN TENTHS	CAMBER %
0	0
1	0·55
2	1·10
3	1·66
4	2·21
5	2·76
7	3·86

FIG. 16. Effect of camber on variation of aerodynamic-centre position with M.

N.A.C.A. 16–X 09 and 16–X 12 aerofoils.

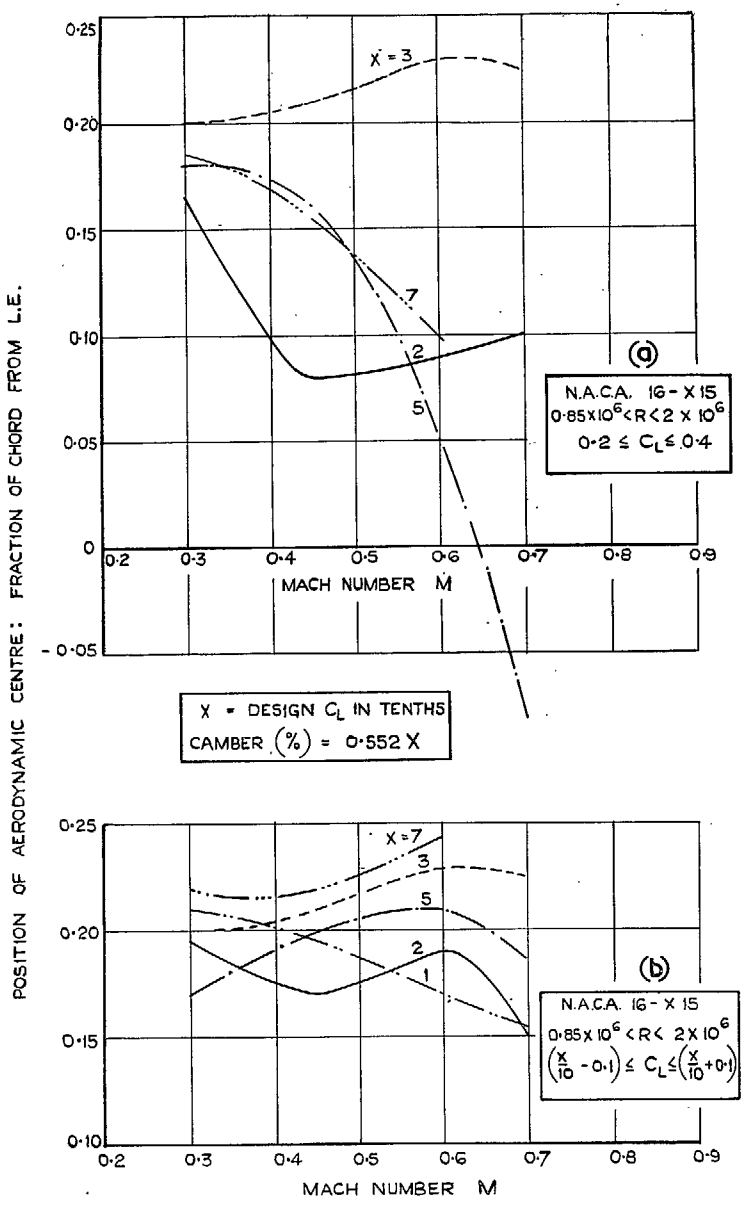

FIG. 17. Effect of camber on variation of aerodynamic-centre position with M.

N.A.C.A. 16–X 15 aerofoils.

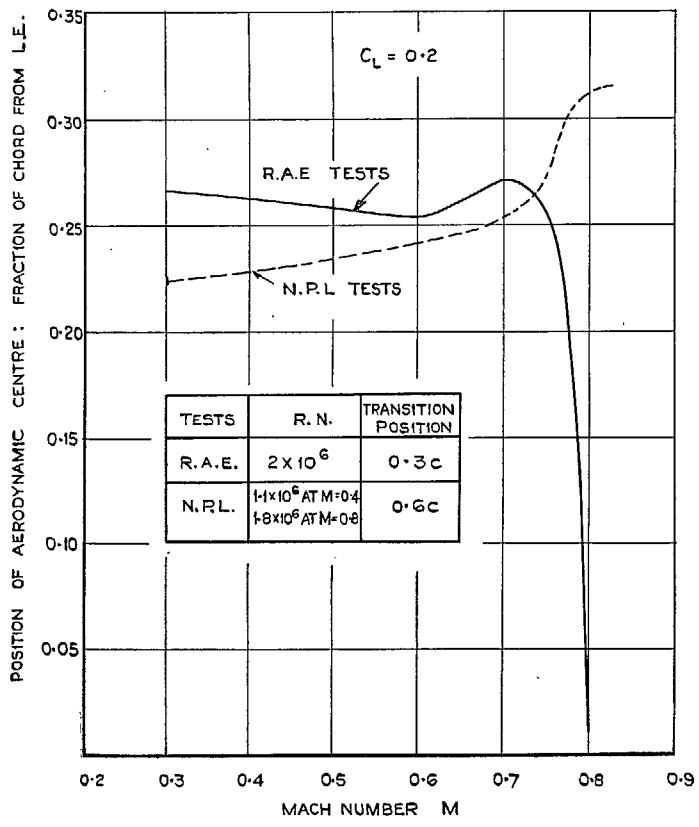

FIG. 18. Comparison of aerodynamic-centre positions as deduced from R.A.E and N.P.L. tests: *Mustang* low-drag section.

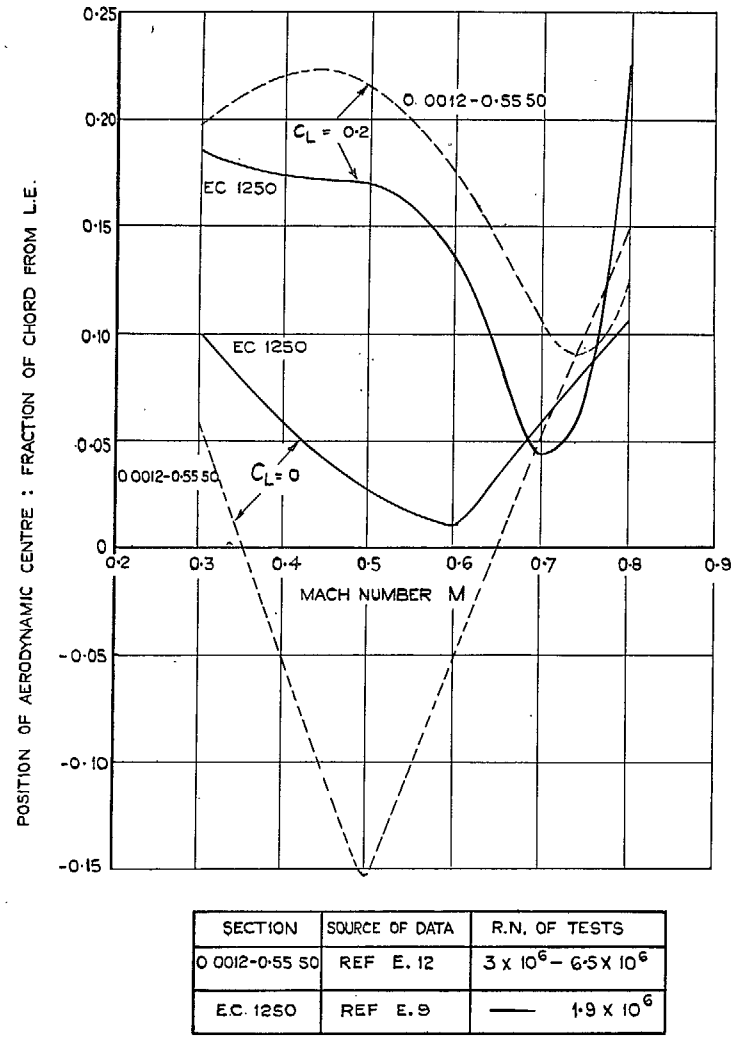

FIG. 19. Variation of aerodynamic centre with Mach number for two similar aerofoils (0 0012-0·55 50 and E.C. 1250).

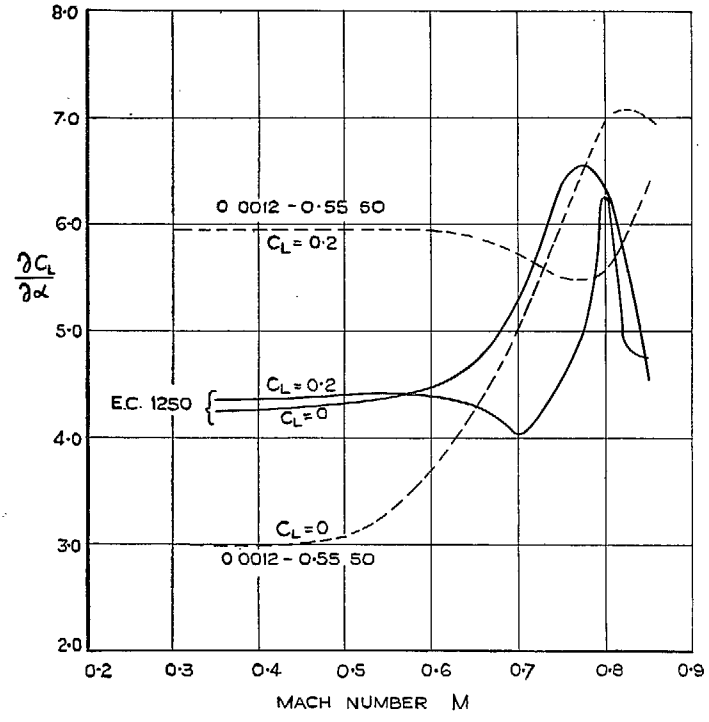

FIG. 20. Variation of lift slope with Mach number for two similar aerofoils (0 0012–0·55 50 and E.C. 1250).

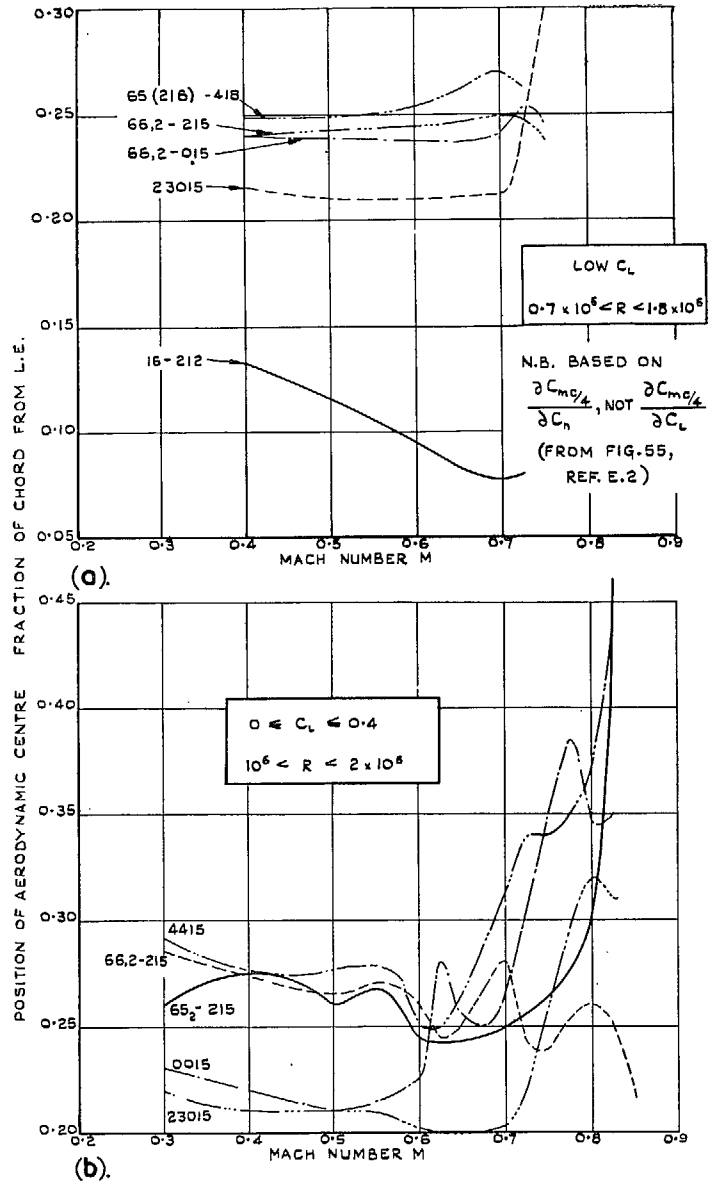

FIG. 21. Variation of aerodynamic centre with Mach number for two miscellaneous collections of N.A.C.A. aerofoils.

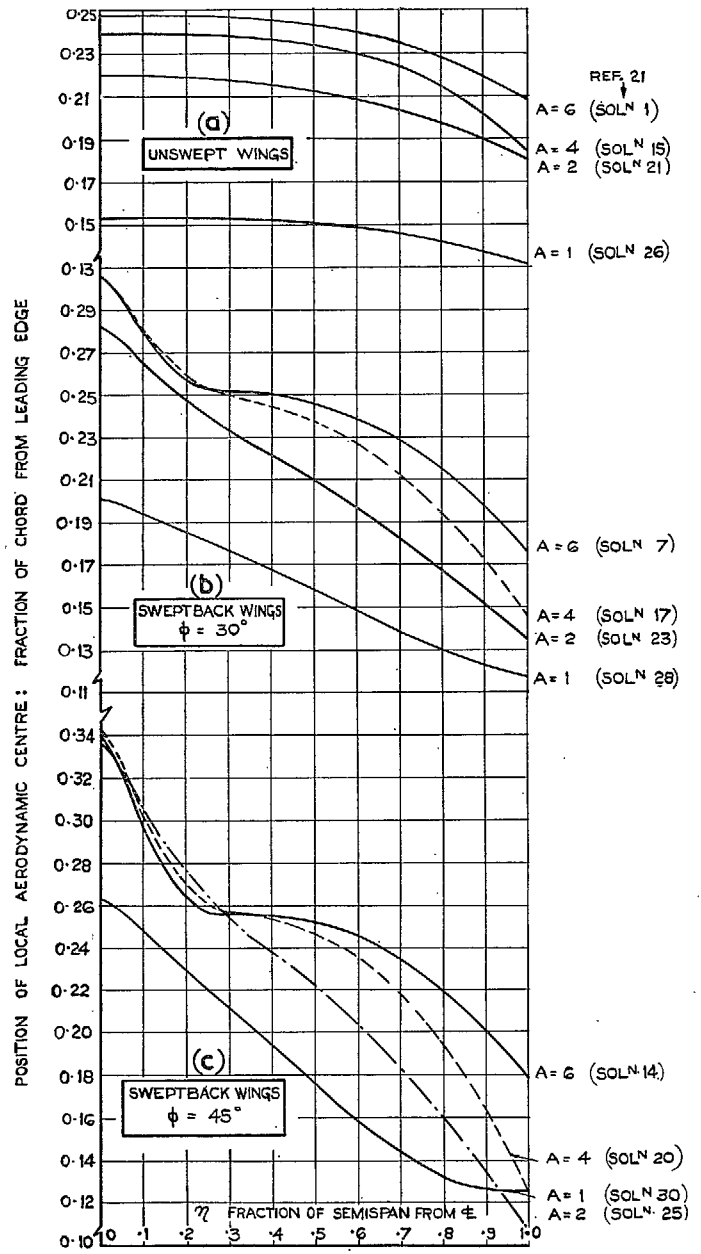

FIG. 22. Local aerodynamic centres for constant-chord wings at uniform incidence (Falkner).

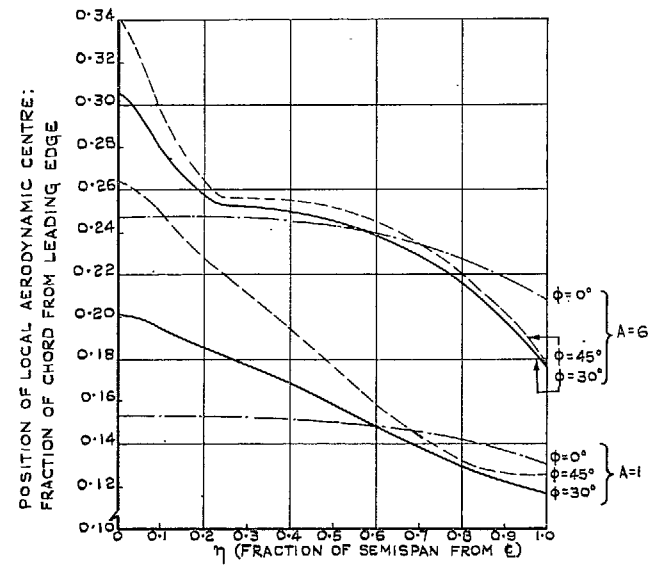

FIG. 23. Effect of sweepback on locus of aerodynamic centres for constant-chord wings of aspect ratios 6 and 1 (Falkner).

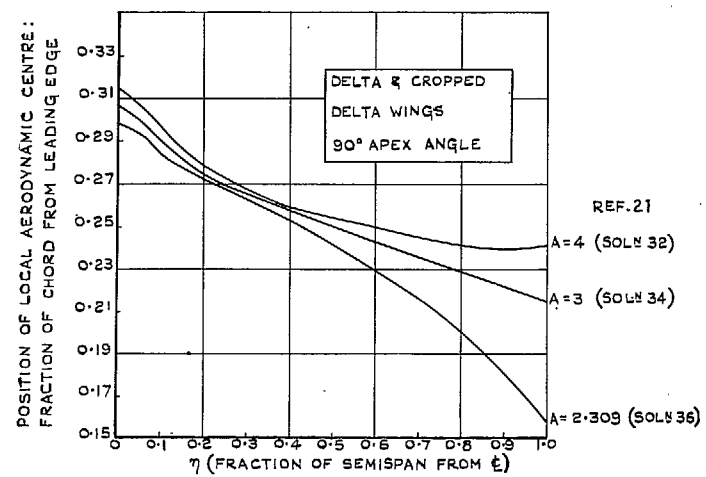

FIG. 24. Local aerodynamic centres for delta and cropped delta wings at uniform incidence (Falkner).

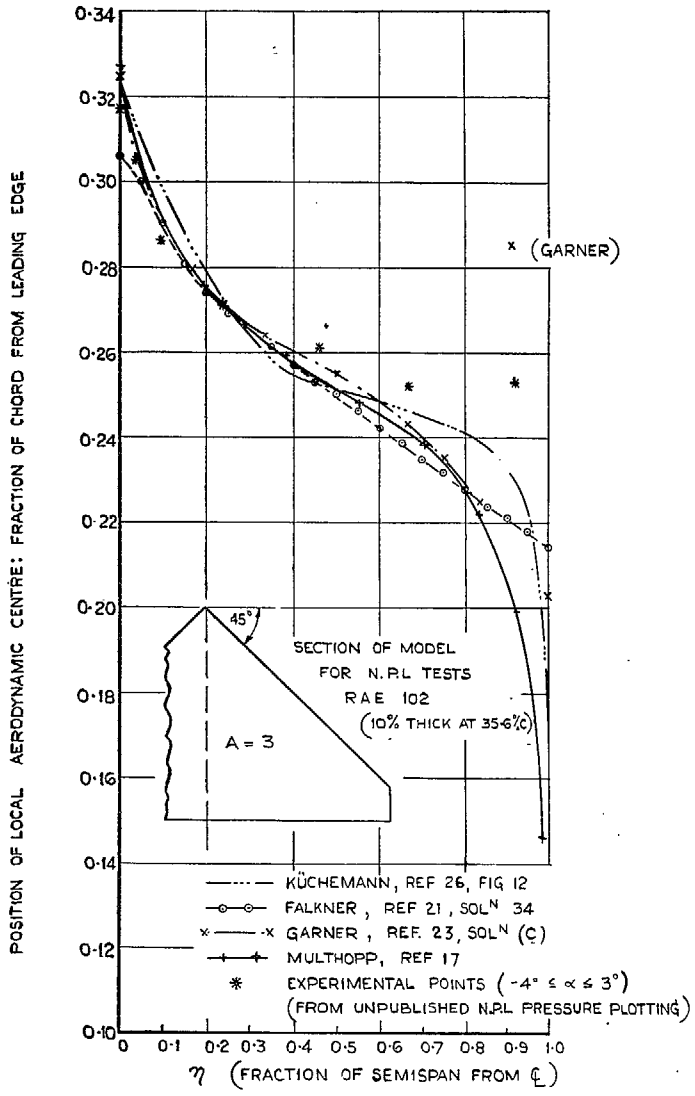

FIG. 25. Comparative calculations of local aerodynamic centre for a delta wing (uniform incidence).

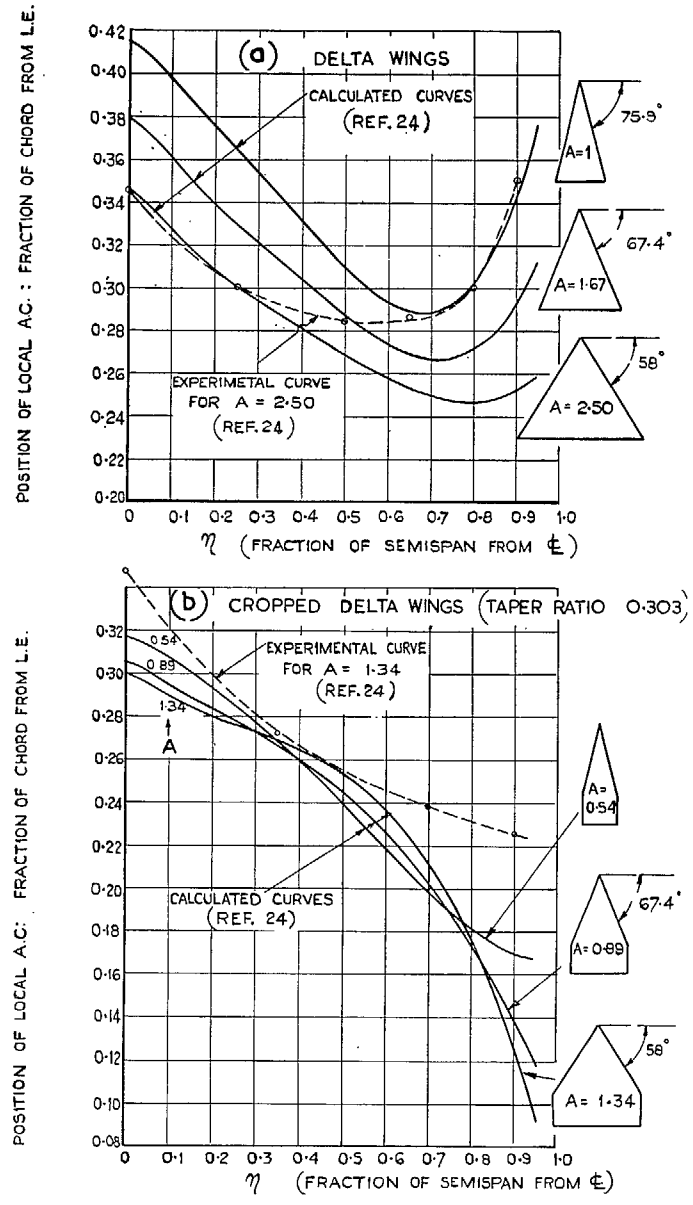

FIG. 26. Local aerodynamic centres of delta and cropped delta wings having various apex angles (uniform incidence).

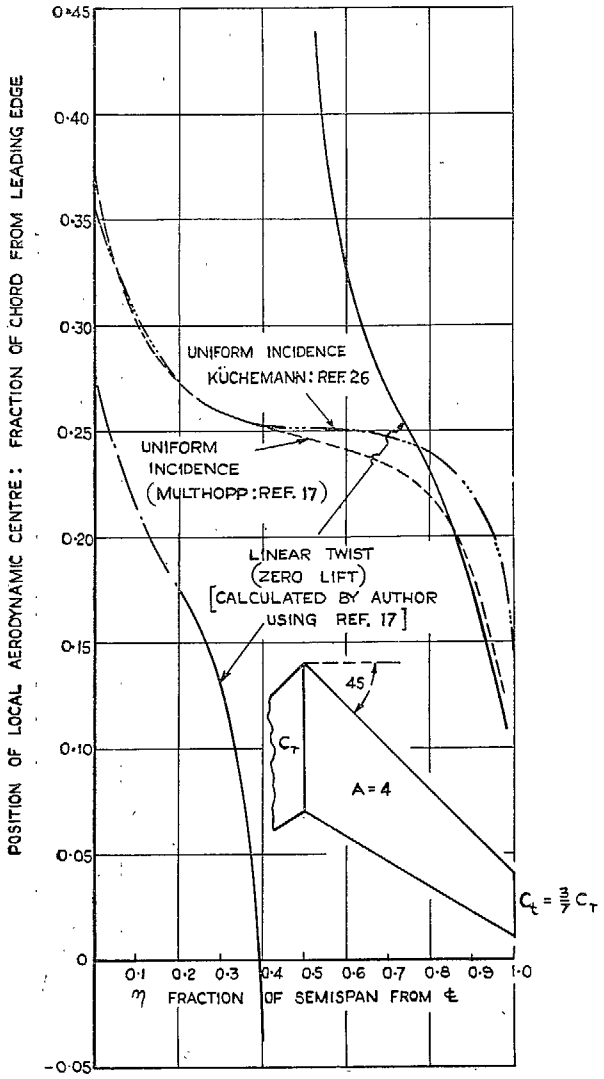

FIG. 27. Calculated local aerodynamic centres for a tapered swept-back wing at uniform incidence and with linear twist at zero lift.

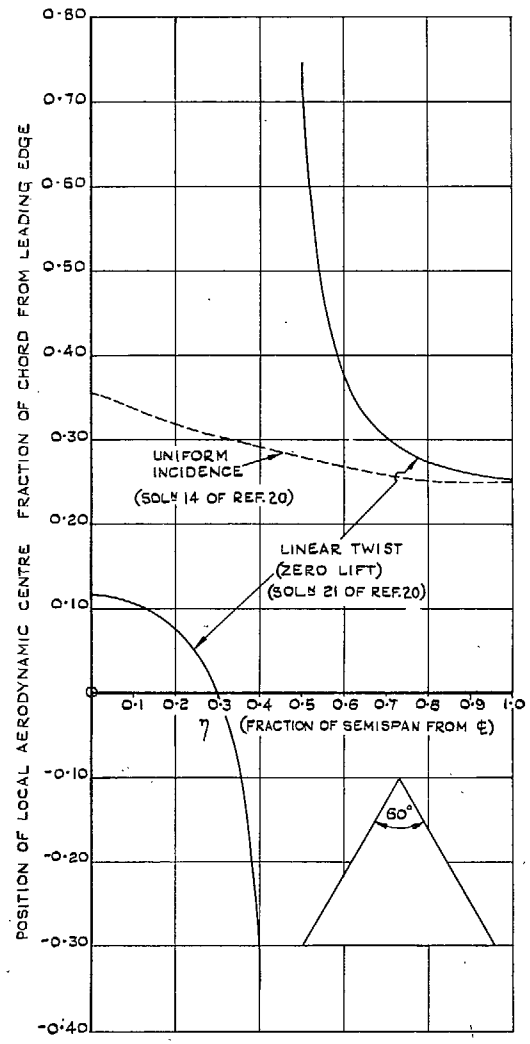

FIG. 28. Local aerodynamic centres for delta wing at uniform incidence and with linear twist at zero lift (Falkner).

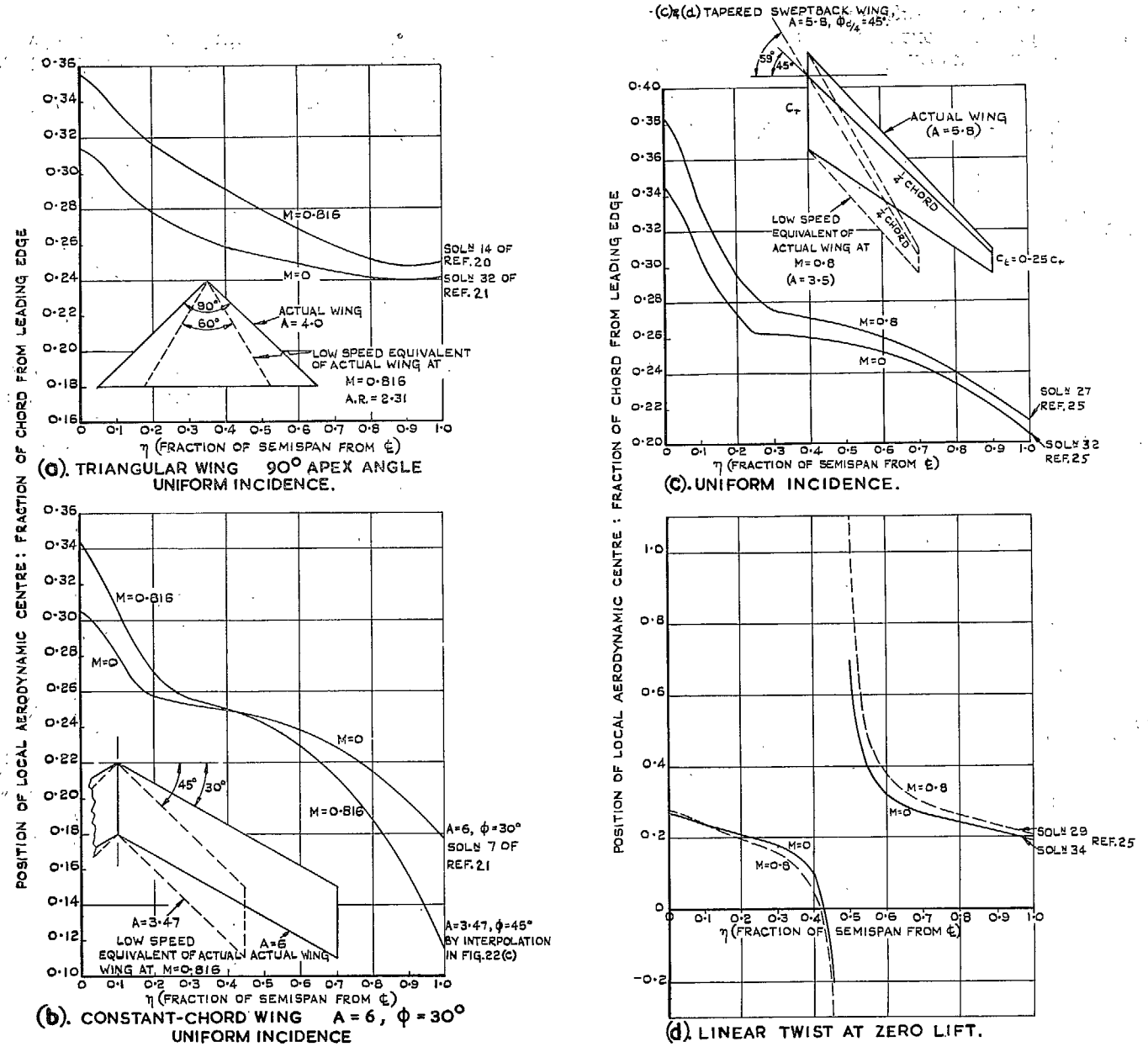

FIG. 29. Effect of compressibility on local aerodynamic centre as deduced from similarity law in conjunction with Falkner's results.

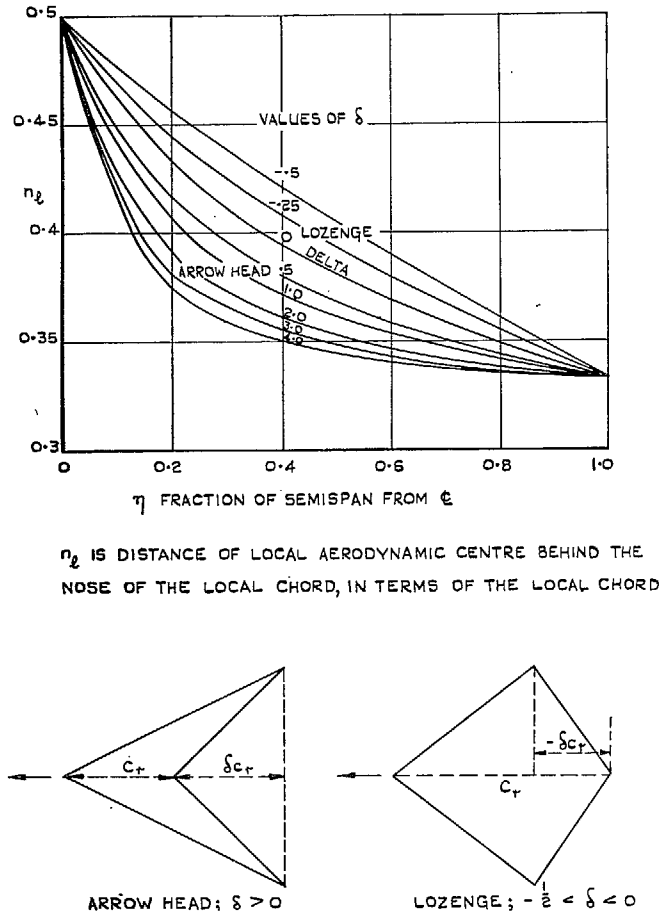

FIG. 30. Supersonic chordwise lift distribution for pointed wings, external solution (from Ref. 1).

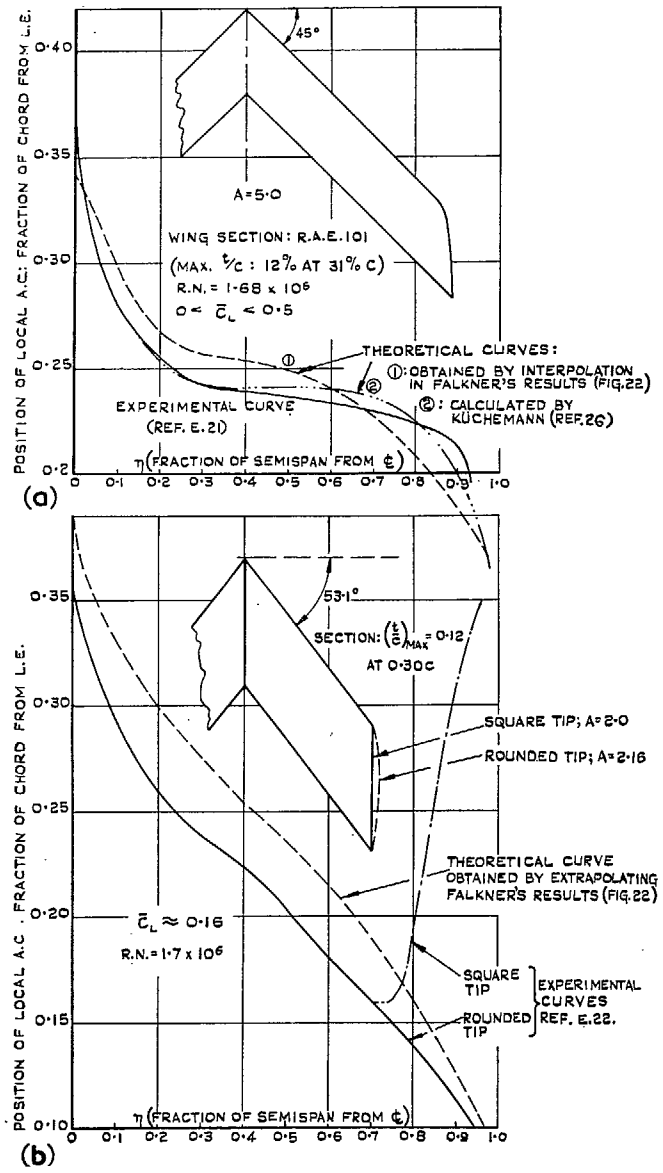

FIG. 31. Comparison of theoretical and experimental results for local aerodynamic centres of two constant-chord swept-back wings.

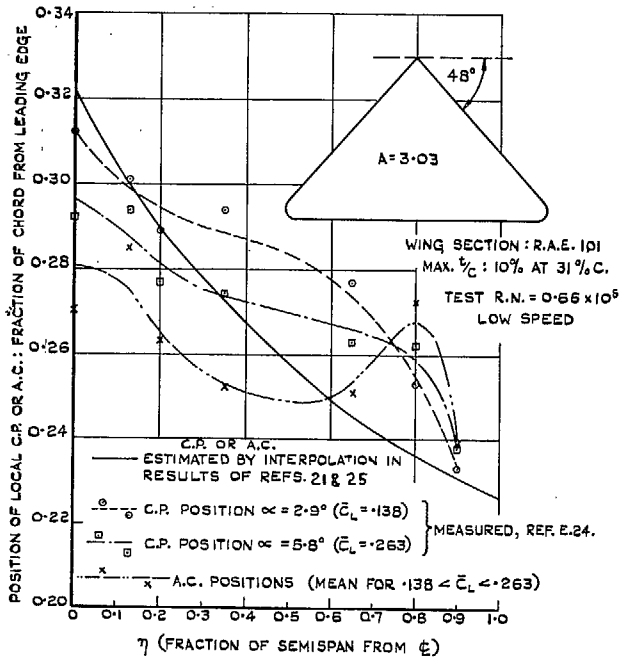

FIG. 32. Local centres of pressure and aerodynamic centres for a delta wing (experimental and theoretical).

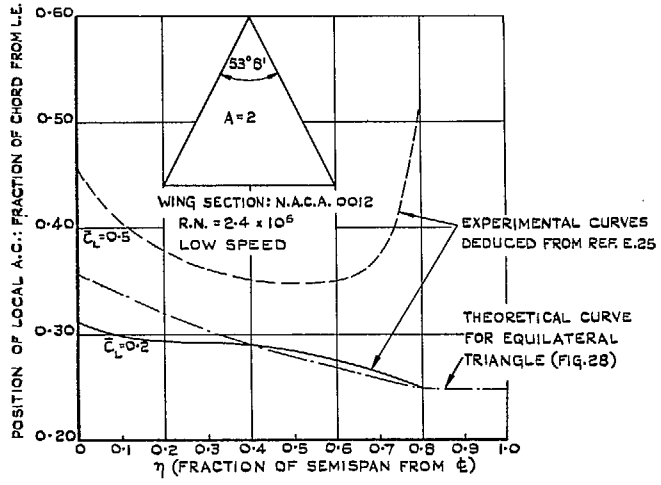

FIG. 33. Local aerodynamic centres of a triangular wing of aspect ratio 2 deduced from low-speed wind-tunnel tests.

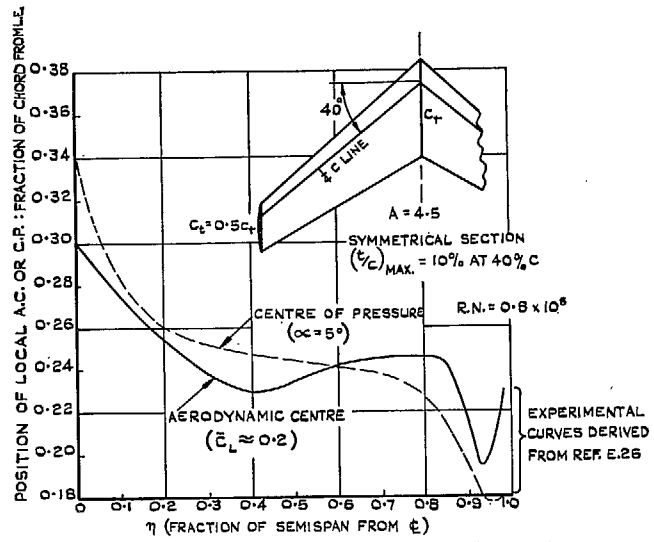

FIG. 34. Local centres of pressure and aerodynamic centres for a tapered swept-back wing as derived from Swedish tests.

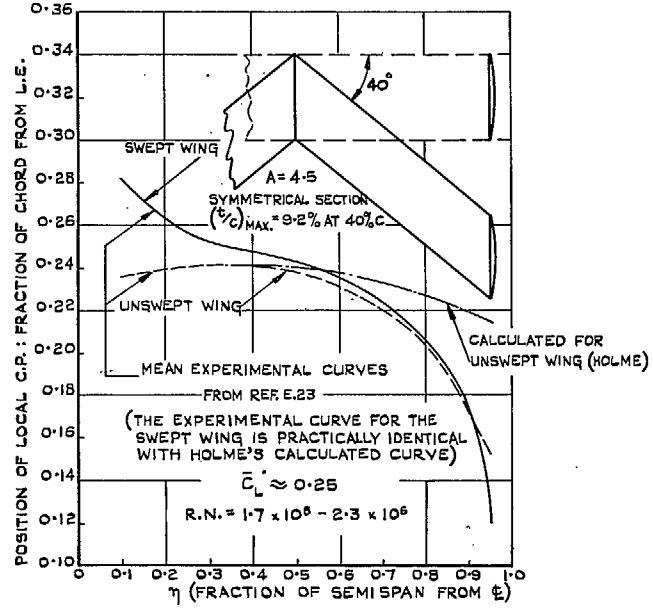

FIG. 35. Comparison of a constant-chord wing of aspect ratio 4·5 and sweepback of 40 deg with an unswept wing of the same aspect ratio.

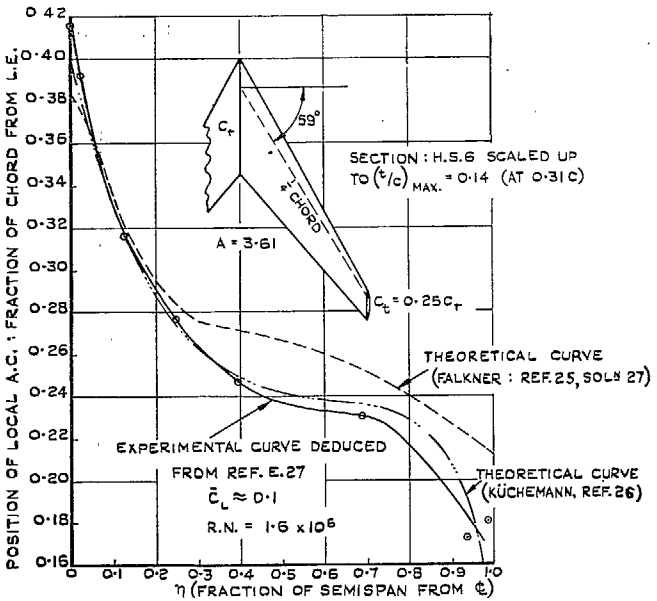

FIG. 36. Experimental and theoretical loci of aerodynamic centres for a tapered swept-back wing.

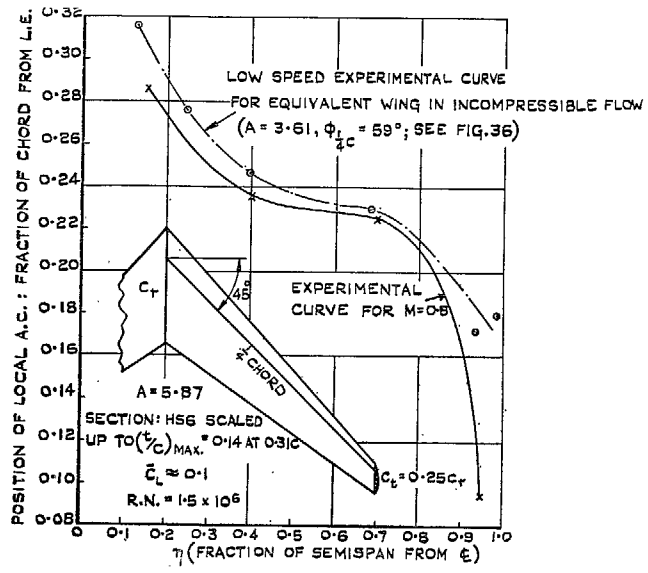

FIG. 37. Experimental comparison of aerodynamic centre positions for a tapered swept-back wing at $M = 0{\cdot}8$ and its low-speed equivalent.

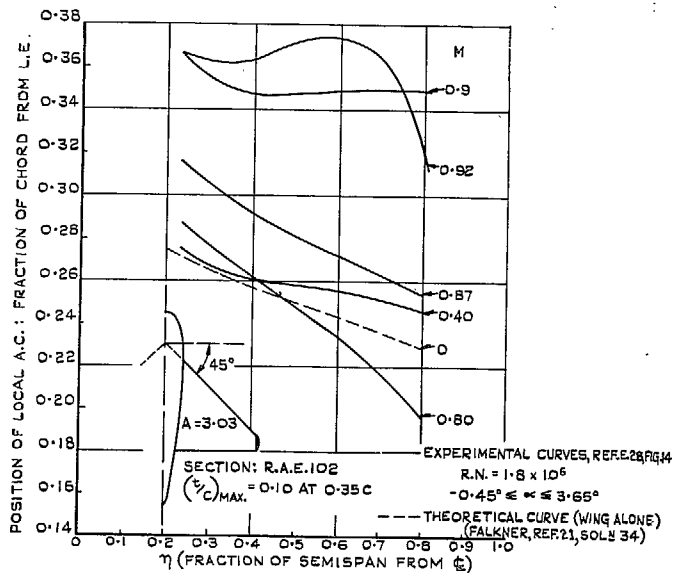

FIG. 38. Effect of compressibility on locus of aerodynamic centres for a delta wing with body.

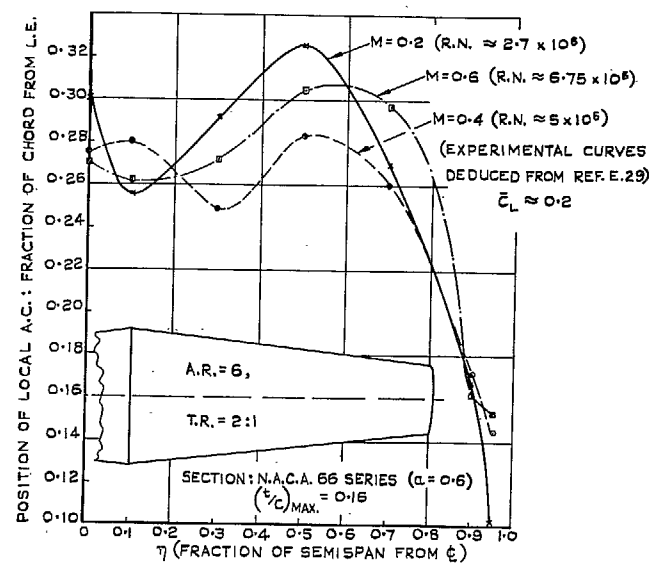

FIG. 39. Effect of compressibility on locus of aerodynamic centres for a tapered wing with unswept half-chord line.

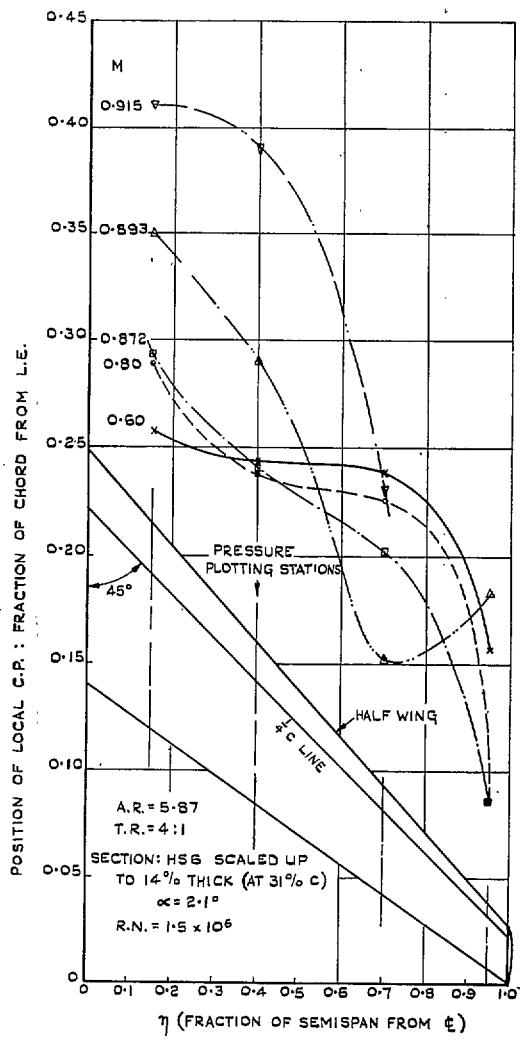

FIG. 40. Effect of compressibility on local centres of pressure of a tapered swept-back wing; $A = 5{\cdot}87$, $\phi_{c/4} = 45$ deg.

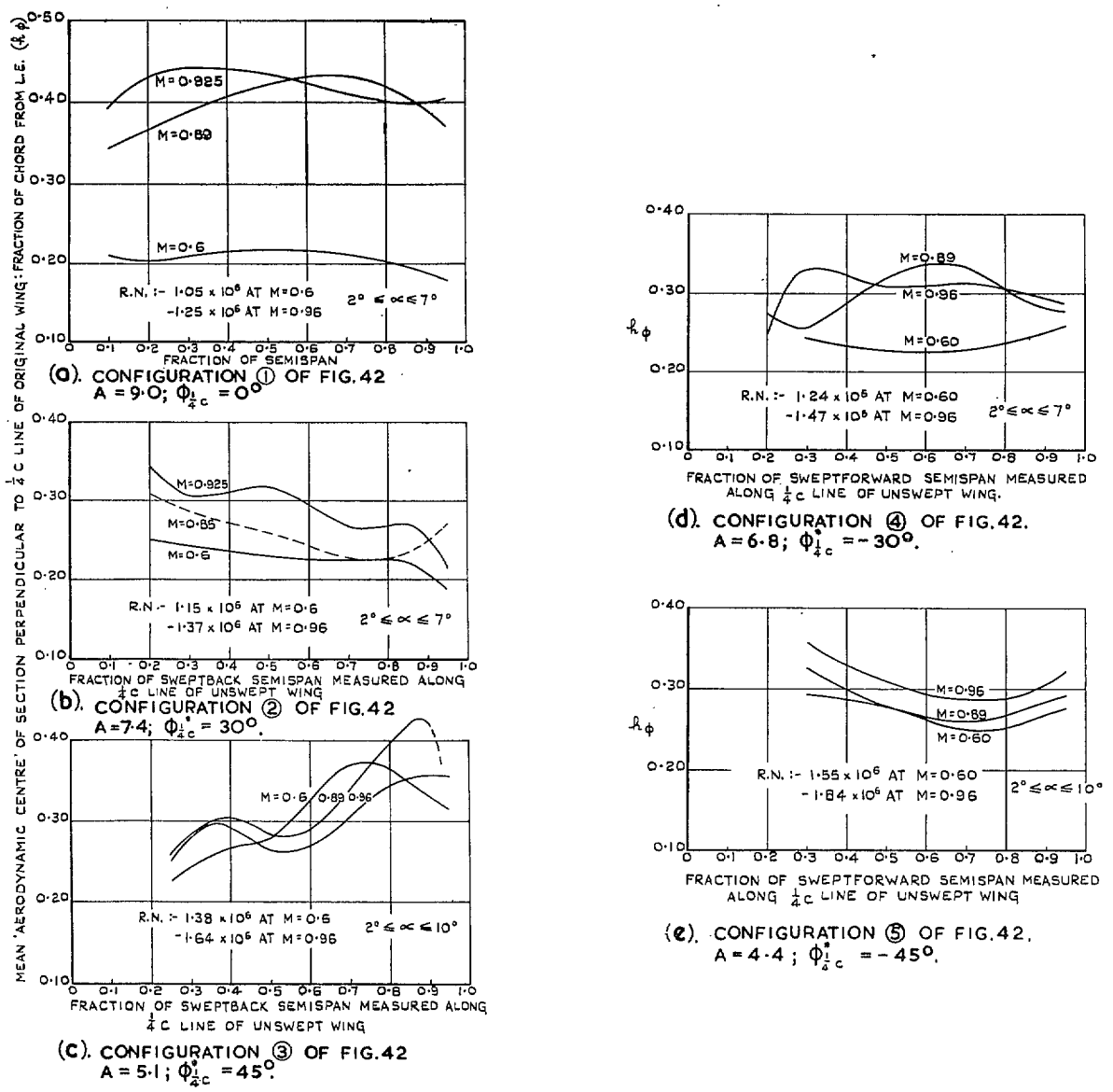

FIG. 41. Effect of compressibility on local ' aerodynamic centres ' of several swept wing plus body configurations.

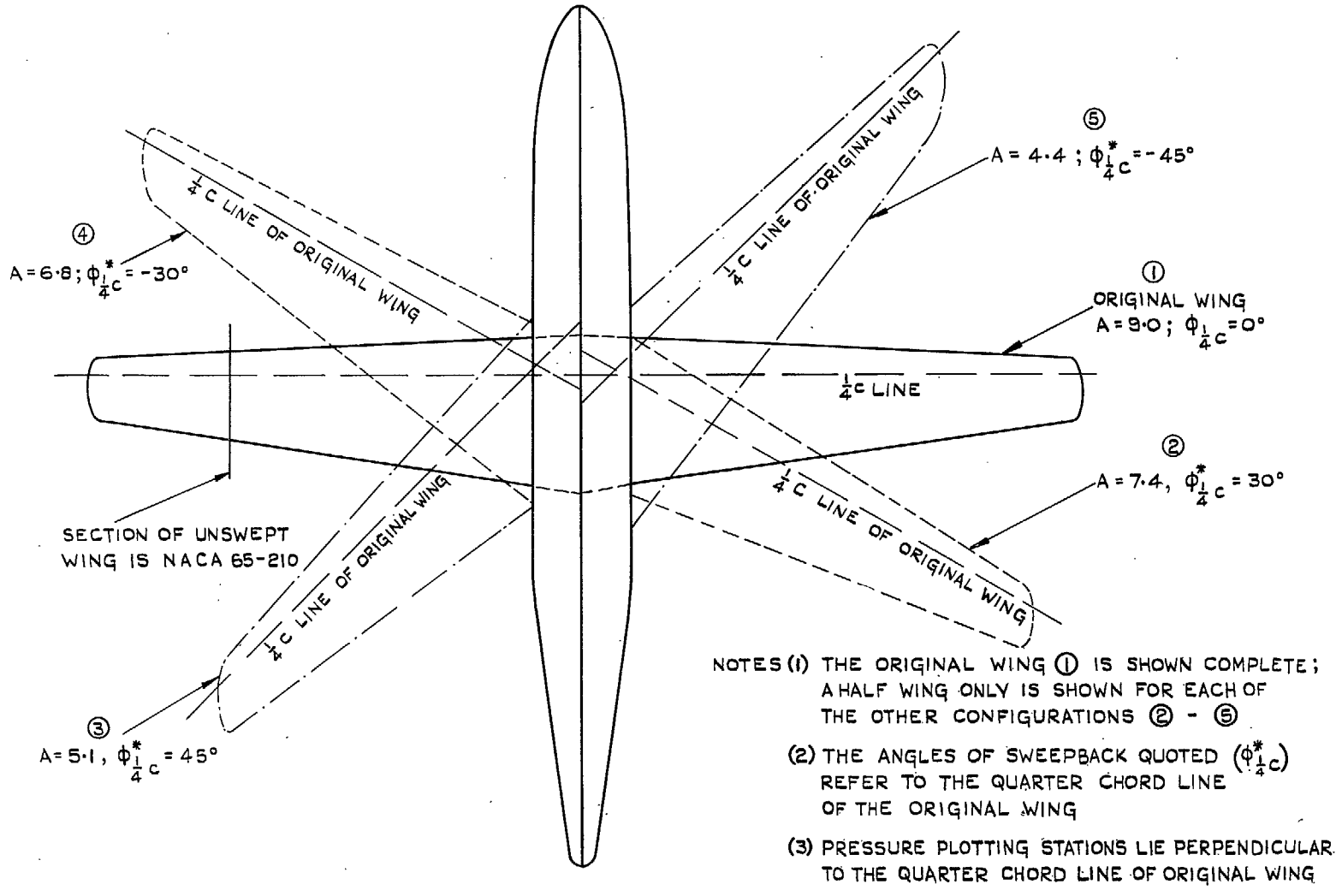

FIG. 42. Test configurations to which the results of Fig. 41 relate.

(4999) WT. 20/9036 K.7 6/57 Hw.

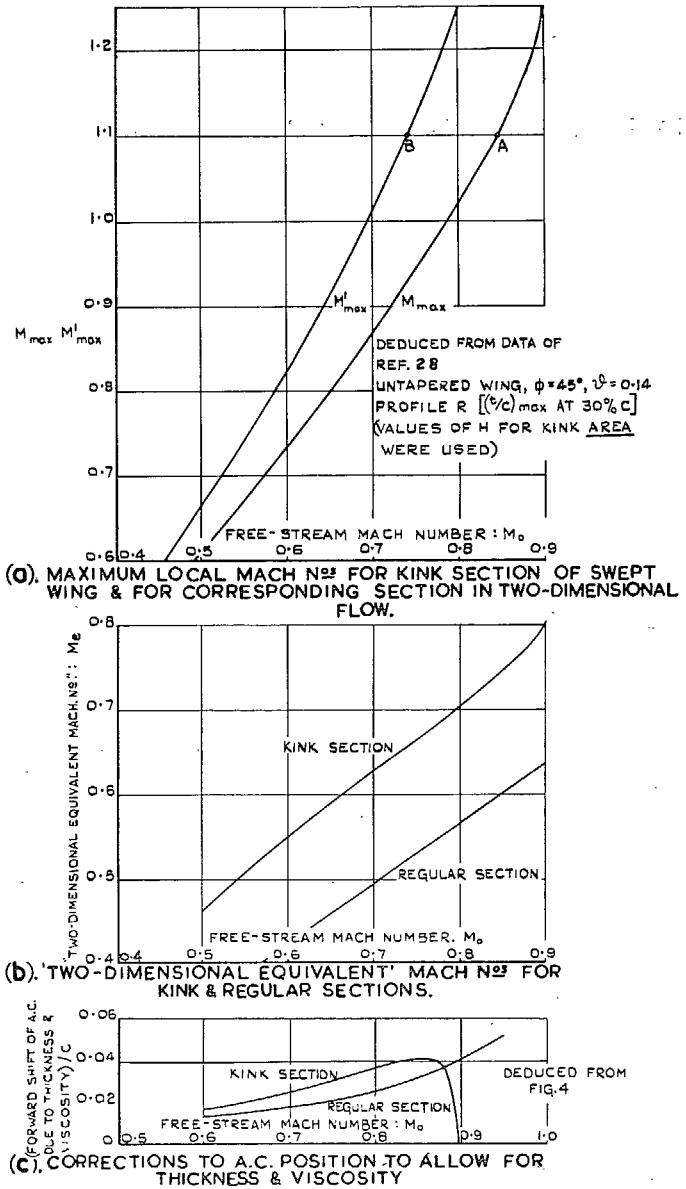

FIG. 43. Derivation of corrections to aerodynamic centres of swept wing to allow for section thickness and viscosity.

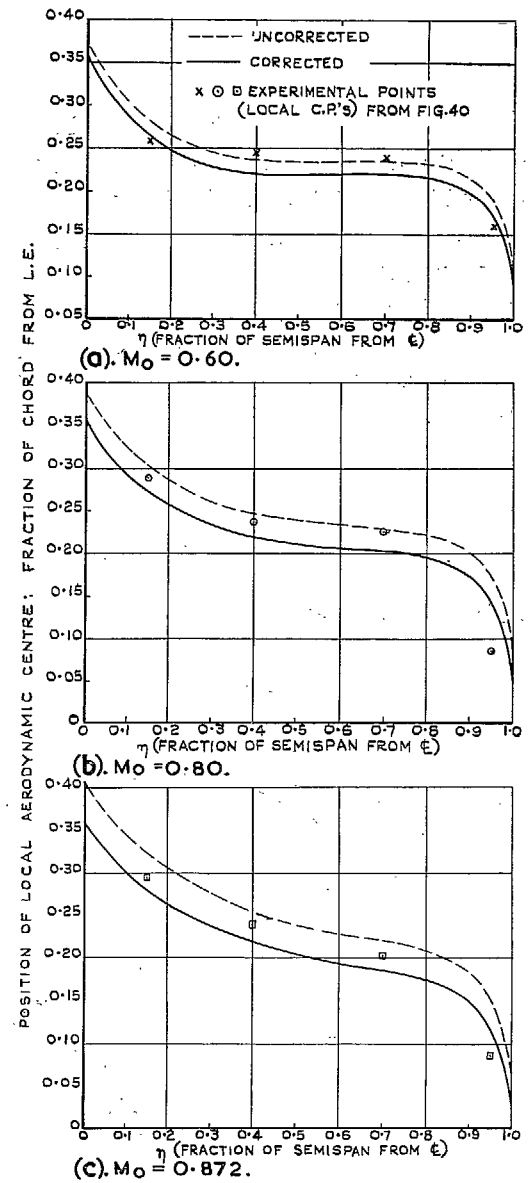

FIG. 44. Calculated aerodynamic centres of the swept-back wing of Fig. 40 with and without correction for section thickness and viscosity.

PRINTED IN GREAT BRITAIN

Publications of the Aeronautical Research Council

ANNUAL TECHNICAL REPORTS OF THE AERONAUTICAL RESEARCH COUNCIL (BOUND VOLUMES)

1939 Vol. I. Aerodynamics General, Performance, Airscrews, Engines. 50*s.* (51*s.* 9*d.*).
Vol. II. Stability and Control, Flutter and Vibration, Instruments, Structures, Seaplanes, etc. 63*s.* (64*s.* 9*d.*)

1940 Aero and Hydrodynamics, Aerofoils, Airscrews, Engines, Flutter, Icing, Stability and Control Structures, and a miscellaneous section. 50*s.* (51*s.* 9*d.*)

1941 Aero and Hydrodynamics, Aerofoils, Airscrews, Engines, Flutter, Stability and Control Structures. 63*s.* (64*s.* 9*d.*)

1942 Vol. I. Aero and Hydrodynamics, Aerofoils, Airscrews, Engines. 75*s.* (76*s.* 9*d.*)
Vol. II. Noise, Parachutes, Stability and Control, Structures, Vibration, Wind Tunnels. 47*s.* 6*d.* (49*s.* 3*d.*)

1943 Vol. I. Aerodynamics, Aerofoils, Airscrews. 80*s.* (81*s.* 9*d.*)
Vol. II. Engines, Flutter, Materials, Parachutes, Performance, Stability and Control, Structures. 90*s.* (92*s.* 6*d.*)

1944 Vol. I. Aero and Hydrodynamics, Aerofoils, Aircraft, Airscrews, Controls. 84*s.* (86*s.* 3*d.*)
Vol. II. Flutter and Vibration, Materials, Miscellaneous, Navigation, Parachutes, Performance, Plates and Panels, Stability, Structures, Test Equipment, Wind Tunnels. 84*s.* (86*s.* 3*d.*)

1945 Vol. I. Aero and Hydrodynamics, Aerofoils. 130*s.* (132*s.* 6*d.*)
Vol. II. Aircraft, Airscrews, Controls. 130*s.* (132*s.* 6*d.*)
Vol. III. Flutter and Vibration, Instruments, Miscellaneous, Parachutes, Plates and Panels, Propulsion. 130*s.* (132*s.* 3*d.*)
Vol. IV. Stability, Structures, Wind Tunnels, Wind Tunnel Technique. 130*s.* (132*s.* 3*d.*)

Annual Reports of the Aeronautical Research Council—

1937 2*s.* (2*s.* 2*d.*) 1938 1*s.* 6*d.* (1*s.* 8*d.*) 1939–48 3*s.* (3*s.* 3*d.*)

Index to all Reports and Memoranda published in the Annual Technical Reports, and separately—

April, 1950 - - - - R. & M. 2600 2*s.* 6*d.* (2*s.* 8*d.*)

Author Index to all Reports and Memoranda of the Aeronautical Research Council—

1909—January, 1954 R. & M. No. 2570 15*s.* (15*s.* 6*d.*)

Indexes to the Technical Reports of the Aeronautical Research Council—

December 1, 1936—June 30, 1939	R. & M. No. 1850	1*s.* 3*d.* (1*s.* 5*d.*)
July 1, 1939—June 30, 1945	R. & M. No. 1950	1*s.* (1*s.* 2*d.*)
July 1, 1945—June 30, 1946	R. & M. No. 2050	1*s.* (1*s.* 2*d.*)
July 1, 1946—December 31, 1946	R. & M. No. 2150	1*s.* 3*d.* (1*s.* 5*d.*)
January 1, 1947—June 30, 1947	R. & M. No. 2250	1*s.* 3*d.* (1*s.* 5*d.*)

Published Reports and Memoranda of the Aeronautical Research Council—

Between Nos. 2251–2349	R. & M. No. 2350	1*s.* 9*d.* (1*s.* 11*d.*)
Between Nos. 2351–2449	R. & M. No. 2450	2*s.* (2*s.* 2*d.*)
Between Nos. 2451–2549	R. & M. No. 2550	2*s.* 6*d.* (2*s.* 8*d.*)
Between Nos. 2551–2649	R. & M. No. 2650	2*s.* 6*d.* (2*s.* 8*d.*)

Prices in brackets include postage

HER MAJESTY'S STATIONERY OFFICE

York House, Kingsway, London W.C.2; 423 Oxford Street, London W.1 (Post Orders: P.O. Box 569, London S.E.1)
13a Castle Street, Edinburgh 2; 39 King Street, Manchester 2; 2 Edmund Street, Birmingham 3; 109 St. Mary Street, Cardiff; Tower Lane, Bristol, 1; 80 Chichester Street, Belfast, *or through any bookseller.*

S.O. Code No. 23-3000